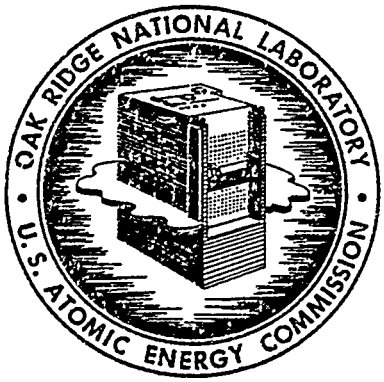

OAK RIDGE NATIONAL LABORATORY

operated by

UNION CARBIDE CORPORATION

for the

U.S. ATOMIC ENERGY COMMISSION

ORNL-TM-15

WASTE TREATMENT AND DISPOSAL

PROGRESS REPORT

FOR JUNE AND JULY 1961

ORNL-TM-15

82

CHEMICAL TECHNOLOGY DIVISION

AND

HEALTH PHYSICS DIVISION

WASTE TREATMENT AND DISPOSAL PROGRESS REPORT FOR JUNE AND JULY 1961

R. E. Blanco and E. G. Struxness

DATE ISSUED

OCT 24 1961

OAK RIDGE NATIONAL LABORATORY

Oak Ridge, Tennessee

Operated by

UNION CARBIDE CORPORATION

for the

U. S. ATOMIC ENERGY COMMISSION

ABSTRACT

High-Level Waste Calcination. Synthetic TBP-25 aluminum nitrate waste was successfully calcined in the large-scale closecoupled continuous evaporator-pot calciner unit (8-in.-dia by 90-in.-high pot). Automatic operation was maintained 90% of the time. A single major evaporator upset occurred because of a plugged liquid level probe and minor fluctuations due to plugs in the pot liquid-level probes. The plugs were easily removed with a water flush. The final cake had a density of 0.56 g/cc and contained < 0.1 to ~ 0.3 wt % mercury and nitrate. The higher analysis was from the center, which was heated to > 485°C but did not reach 900°C as in the outer zone.

Waste oxides from TBP-25 waste were incorporated into glassy materials after the addition of phosphate and borate fluxing agents. Melts formed at 850 to 950°C were glassy solids when cooled and had densities from 2.41 to 2.47 g/ml. Waste volume reduction factors were from 7.6 to 9.3. The condensate from semicontinuous evaporation of simulated Purex waste made 0.8 M in phosphite contained 1.31% of the ruthenium present. The condensate from batch evaporation of Purex waste made 1.5 M in sodium hypophosphite contained 5.4% of the original ruthenium while the condensate from a similar evaporation of waste made 1.5 M in monobasic sodium phosphate contained 15.1%. Less ruthenium was in the condensate (6.4 vs 7.8%) from batch evaporation when the Purex waste contained 0.8 M hypophosphite than when it contained 0.8 M phosphite. The principal gaseous product from the reaction between 1.5-6 M HNO_3 and 1 M phosphorous acid appeared to be NO. The oxidation of phosphite was catalyzed by certain cations, e.g., mercury.

Objectives and initial design concepts were established for the calcination pilot unit to be installed in the ICPP pilot plant. A contract is being negotiated with Georgia Nuclear Laboratory (Lockheed Nuclear Company) to evaluate alternative mechanical features of the calcination unit.

Low-Level Waste Treatment. A third demonstration run was completed in the small (60 liters/hr) scavenging-ion exchange pilot plant on ORNL low-activity waste. Decontamination factors were satisfactory after 1500 resin bed volumes of waste had been treated, i.e., Sr > 1000, TRE 100, Cs > 100, and sufficiently high for other activities that the waste activity was reduced to < 10% of MPC.

Construction of the large (10 gal/min) pilot plant is close to completion. The scavenging equipment will be tested starting Sept. 1, 1961. A major change to the polishing filter system was made by substituting vertical granular bed pressure filters for the plate and frame filter originally proposed.

The physical properties of vermiculite, clinoptilolite, and rock phosphate were found to be suitable for second-stage treatment of process waste. Since sodium hydroxide treatment of vermiculite ore causes some breakdown of the material, the use of mechanically cleaned ore will be necessary. Design was completed and construction begun on the 3-gal/min pilot plant to demonstrate the effectiveness of mineral column treatment of Process Waste Water Treatment Plant effluent.

Engineering, Economic, and Hazards Evaluation. A cost study of the conversion of high-level solutions to solids by pot calcination was completed. Costs were calculated for processing Purex and Thorex wastes in acidic and reacidified (after alkaline storage) forms and for producing a Thorex glass from acidic waste. Aging had a negligible effect on costs for processing in a given vessel size. Aging permits larger vessels to be used, however, and costs for processing in 6-in.-dia vessels were 2 to 3 times as high as for processing in 24-in.-dia vessels. The lowest cost was 0.87×10^{-2} mill/kwh$_e$ for processing acidic Purex and Thorex wastes in 24-in.-dia vessels, and the highest was 5.0×10^{-2} mill/kwh$_e$ for processing reacidified Purex and Thorex wastes in 6-in.-dia vessels. About 7 years interim liquid storage would be required before acidic Purex waste could be processed in 24-in.-dia vessels.

Disposal in Deep Wells. Test drilling at the site of the second fracturing experiment is nearly completed. The upper grout sheet, composed of four separate layers formed one above the other, extends out from the injection well some 500 ft to the east and northeast, but only short distances out in other directions. The lower grout sheet extends largely to the north and northwest, but its outer limits are still undefined.

The 3000-ft core hole at the proposed site of the Waste Disposal Fracturing Plant is now at about 2200 ft. Rock well suited to disposal operations has been encountered from 1500 ft to the present bottom of the hole.

Disposal in Natural Salt Formations. Stress measurements in the pillars of the Hutchinson mine have shown the absence of horizontal stresses and the presence of vertical stress varying from 1300 to 1600 psi. The absence of horizontal stress was expected; however, the theoretical stress in the pillars based on mine depth and percentage salt extraction should have been about 1950 psi.

Comparison of the data from the field cavities and theoretical calculations of temperature rises around spheres indicates that the thermal conductivity of the salt surrounding the experimental cavities is 2.6 Btu hr^{-1} ft^{-1} $^{o}F^{-1}$ and the diffusivity is 0.099 ft^2/hr. These values agree quite well with the Birch values for single pure-salt crystals at 80 and 65°C, respectively.

A computer code was designed for the solution of temperature rises in a heat-generating layer of infinite horizontal dimensions (flat slab) and in the salt surrounding the layer, as a function of time for wastes of variable age. The use of this code showed that the storage of waste decayed less than one year is wasteful of mine space and that the thickness of the slab (1-10 ft) has little effect on the temperature rise in the slab.

Studies on radiolytic gas production of wastes in salt showed that gas production can be eliminated by pressurizing the cavity or by maintaining an atmosphere of hydrogen over the waste. The pressures involved are not extremely high (3-10 atm), but they represent a problem in cavity design.

Disposal of liquids in salt as a mixed layer of salt and waste appears to eliminate the problems of radiolytic off-gas, as well as cavity alteration.

Clinch River Studies. A continuous water-sampling system was installed at Centers Ferry on the Clinch River. With the assistance of the ORNL Instrumentation and Control Division, the instruments were so designed that the rate of sampling is proportional to the velocity of flow in the river.

Results of sorption tests on membrane filters indicate that essentially no strontium, cobalt, or ruthenium is sorbed as river water samples are filtered. A small percentage of cesium, 4%, is sorbed by the filters.

Various types of bottom sediment core samplers were tested and evaluated for compaction and retention characteristics. The most effective sampler was a 3.5-in.-dia split-tube sampler with basket shoe.

Results of a recent TVA silt range survey of the Clinch River showed that additional cross section sampling sections, intermediate to the standard silt ranges, do not significantly change estimates of sediment volume.

Fundamental Studies of Minerals. Sodium-vermiculite showed three distinct sorption-of-strontium responses in the pH range 2 to 11. Up to pH 4.5 the response depends on the displacement of aluminum from octahedral layers of the mineral. Thus, sorption was $< 10\%$ at pH 2 and only 59% at pH 4.0; in both cases sorption was maximum after contact for less than 96 hr. Sorption increased uniformly (to $\sim 70\%$) between pH 4.5 and 9.0 up to 96 hr contact. At pH 11 sorption sharply increases to 91% after 96 hr.

Comparison of strontium removal by sodium-vermiculite, clinoptilolite, Duolite C-3, and Dowex 50 showed that sodium-vermiculite is ineffective at low pH but competitive at basic pH's. Exchange capacity and stability at low pH are important considerations in strontium sorption reactions.

Particle diffusion processes have a pronounced influence on cesium breakthrough curves from small columns operated for rather short times. Extrapolation from bench-scale experiments to the field may require correction for this phenomenon, as the cesium loading increases with increased time of column operation. For prolonged column operation times, the effects of particle diffusion are not so pronounced. The choice of particle size for an operating column may be determined, in part at least, by the kinetics of the exchange reaction.

White Oak Creek Basin Study. An investigation was started to determine the vertical and lateral distribution of radionuclides in the bed of former White Oak Lake. Preliminary results from core samples taken along transects at the lower and upper ends of the lake indicate more gamma activity per gram at the upper transect than at the lower one, most of the gamma activity contained in the first 12 in. of soil, and activity in the upper few inches of each core rather uniformly distributed.

CONTENTS

1.0 INTRODUCTION

This report is the second of a series of bimonthly reports on progress in the ORNL development program, the objective of which is to develop and demonstrate on a pilot plant scale integrated processes for treatment and ultimate disposal of radioactive wastes resulting from reactor operations and reactor fuel processing in the forthcoming nuclear power industry. The wastes of concern include those of high, intermediate, and low levels of radioactivity in liquid, solid, or gaseous states.

Principal current emphasis is on high- and low-level liquid wastes. Under the integrated plan, low-level wastes, consisting of very dilute salt solutions, such as cooling water and canal water, would be treated by scavenging and ion exchange processes to remove radioactive constituents and the water discharged to the environment. The retained waste solids or slurries would be combined with the high-level wastes. Alternatively, the retained solids or the untreated waste could be discharged to the environment in deep geologic formations. The high-level wastes would be stored at their sites of origin for economic periods to allow for radioactive decay and artificial cooling. Interim storage and cooling, which can be accomplished safely in conventional storage tanks, greatly simplify the problems of subsequent handling and should decrease the overall cost of waste management. Studies (1) have shown that the cost of permanent tank storage may not be excessive, but its safety is questionable.

Alternative methods to tank storage for ultimate treatment and disposal are being investigated to find safer and possibly cheaper methods. One approach is to convert the liquids to solids by high temperature "pot" calcination or fixation in the final storage container (pot) itself and store it in a permanently dry environment such as a salt mine. This is undoubtedly the safest method since complete control of radioactivity can be ensured within present technology during treatment, shipping, and storage. Another approach is to dispose of the liquid directly into sealed or vented salt cavities. Research and development work is planned to determine the relative feasibility, safety, and economics of these methods, although the major effort will be placed on conversion to solids and final storage as solids.

Tank storage or high-temperature calcination of intermediate-level wastes may be unattractive because of their large volumes. Consequently, other disposal methods will be studied. One method, e.g., addition of solidifying agents prior to direct disposal into impermeable shale by hydrofracturing, is under investigation at present. Particular attention is given to the engineering design and construction of an experimental fracturing plant to dispose of ORNL intermediate-level wastes by this method if proved feasible.

Environmental research on the Clinch River, motivated by the need for safe and realistic permissible limits of waste releases, is included in this program. The objective is to obtain a detailed characterization of fission product distribution, transport, and accumulation in the physical, chemical, and biological segments of this environment.

2.0 HIGH-LEVEL WASTE CALCINATION

The pot calcination process for converting high-activity-level wastes to solids is being studied on both a laboratory and engineering scale to provide design information for construction of a pilot plant. Development work has been with synthetic Purex, Darex, and TBP-25 wastes containing millicurie amounts of ruthenium but has not been demonstrated on actual high-activity-level wastes. A general flowsheet was shown previously (2).

2.1 Evaporation-Calcination (J. C. Suddath, C. W. Hancher, L. J. King)

Two large-scale waste calcination runs were made in the close-coupled evaporation-calciner (2-4) with an 8-in.-dia by 90-in.-high stainless steel calcination pot. Run R-39, with simulated TBP-25 waste as fuel, was a duplicate of R-38 (5) to establish reproducibility of results. Run R-40, with simulated Purex waste to which MgO had been added to decrease sulfate volatility, was a duplicate of R-37 where calciner pot corrosion was severe (2,6). Although in run R-40 temperature was carefully controlled to maintain it below 900°C at all points, corrosion was again severe. Therefore, magnesium will not be used as an additive pending further laboratory-scale evaluation. Complete details of R-40 are not yet available.

Run R-39. The composition of the feed in run R-39 simulated that of the TBP-25, aluminum-bearing, wastes stored at the Idaho Chemical Processing Plant (Table 2.1). Nonradioactive ruthenium was added to determine its volatility under test conditions. Material balances for nitrate, mercury, and ruthenium were 94.5%, 63.6%, and 83.4%, respectively (Table 2.2). Only 2% of the mercury fed to the system remained with the calcined solids. However, 77% of the ruthenium remained with the calcined solid. The pot off-gas line contained a solid film which was 90% mercury and 1% ruthenium. The material unaccounted for probably plated out on metal surfaces in the system. The ruthenium concentration in the evaporator condensate was below detection.

Table 2.1 Composition of Simulated TBP-25 Waste Used in Evaporation-Calcination Run R-39

	H^+ (M)	Al^{3+} (M)	Hg^{++} (g/liter)	NO_3^- (M)	Fe^{3+} (g/liter)	Na^+ (g/liter)	Ru (g/liter)
As made up	1.26	1.72	4.0	6.6	0.16	2.4	-
As analyzed							
(Tank 1)	1.70	1.76	4.00	7.02	0.214	-	0.113
(Tank 2)	1.71	1.75	3.95	7.04	0.217	-	0.173
(Tank 3)	1.69	1.77	3.98	7.08	0.242	-	0.151

Table 2.2 Material Balances in Test R-39

Input		Recovery	
	Nitrate		
3227 g moles	Evaporator condensate	2823 g moles	87.48%
	Solid	0.7 g moles	0.02
	Off-gas	40 g moles	1.20
	Evaporator heel	187.7 g moles	5.82
			94.52%
	Ruthenium		
0.685 g moles	Evaporator condensate	Below detection	
	Solid	0.529 g moles	77.23%
	Evaporator heel	0.042 g moles	6.13
			83.36%
	Mercury		
9.29 g moles	Evaporator condensate	1.77 g moles	19.05%
	Solid	0.18 g moles	1.94
	Evaporator heel	3.96 g moles	42.63
			63.62%
	Off-gas		
	Total	797 cu ft	
	Leakage and purge	663 cu ft	
	Noncondensable	134 cu ft	
	(102 cu ft oxygen)	134/489 = 0.274 cu ft/liter of system feed	

The run started with the evaporator filled with cold feed and the calciner empty and cold. The evaporator contents were heated to boiling and then the calciner was heated and filled simultaneously over a 30-min period. As the control variables reached set point conditions, they were switched from manual to automatic control. The rate of water addition to the evaporator, which averaged 30.6 liters/hr, was controlled manually during most of the run to find the temperature at which the acidity of the pot would not exceed 6 M, so that ruthenium volatility would be minimum. A liquid temperature of 117°C was chosen after laboratory analyses had been made during the run, but later analyses showed that the average acidity was 1 M. Consequently, much less water could have been added if a higher set point temperature had been maintained. The water to feed ratio was 7.4/1. A 3 to 1 ratio, at a vapor temperature of 111°C, would be nearer ideal.

Automatic control was satisfactory within the prescribed limits during 90% of the feeding period. In a single upset, an evaporator level control probe became plugged, causing a rise in liquid level. The plug was easily removed by flushing the probe with water. However, the valve between the evaporator and the pot continued to cycle between 0 and 40% open, causing about 5% fluctuation in the evaporator controls. Minor plugging of the pot liquid level probe also occurred but was easily cleared with a water flush.

The calciner pot showed no signs of corrosion on the inside, and the outside showed no signs of corrosion or oxidation scaling. A nitrogen purge of 10 cu ft/hr was used between the calciner pot and furnace liner.

The final calcined solid, 33.2 kg, obtained from 489 liters of waste had a bulk density of 0.56 g/ml, including void volume; it was light gray and very crumbly. About 90% of the pot was filled with solids, a hole down the center indicating radial growth. The nitrate and mercury content of the solid varied from 0.1 to 0.38 wt % (Table 2.3). The higher values are from zones where the temperature did not exceed 485°C and the lower from zones that reached 850-900°C.

Table 2.3 Analysis of Solids from R-39

	Amount (wt %)			
	Al	Hg	NO_3	Ru
Top	50.6	0.007	< 0.1	0.17
Middle	45.5	0.32	0.38	0.17
Bottom	50.4	0.007	< 0.1	0.15

2.2 Fixation in Glasses (W. E. Clark, H. W. Godbee, and K. L. Servis)

Simulated TBP-25 waste was incorporated into melts at 850-950°C. On being cooled and either quenched or annealed, the melts gave glassy solids with densities from 2.41 to 2.47 g/cc, representing volume reduction factors of from 7.6 to 9.3. One of the more satisfactory products, based on softening point, fluidity, and quality of final product, contained 38.9, 31.6, 22.9, and 6.5 wt %, respectively, of P_2O_5, Al_2O_3, Na_2O, and B_2O_3 (Table 2.4, melt 1, and Fig. 2.1).

Fluxing agents used to form melts were borate and phosphate. Borate, which was added as tetraborate, $B_4O_7^{=}$, tends to lower the softening point and viscosity of melts; however, it also tends to cause foaming before the solids soften. Phosphate was added as the acid phosphate or hypophosphite, $H_2PO_2^-$, the latter serving as a source of phosphate as well as a reducing agent to control ruthenium volatility.

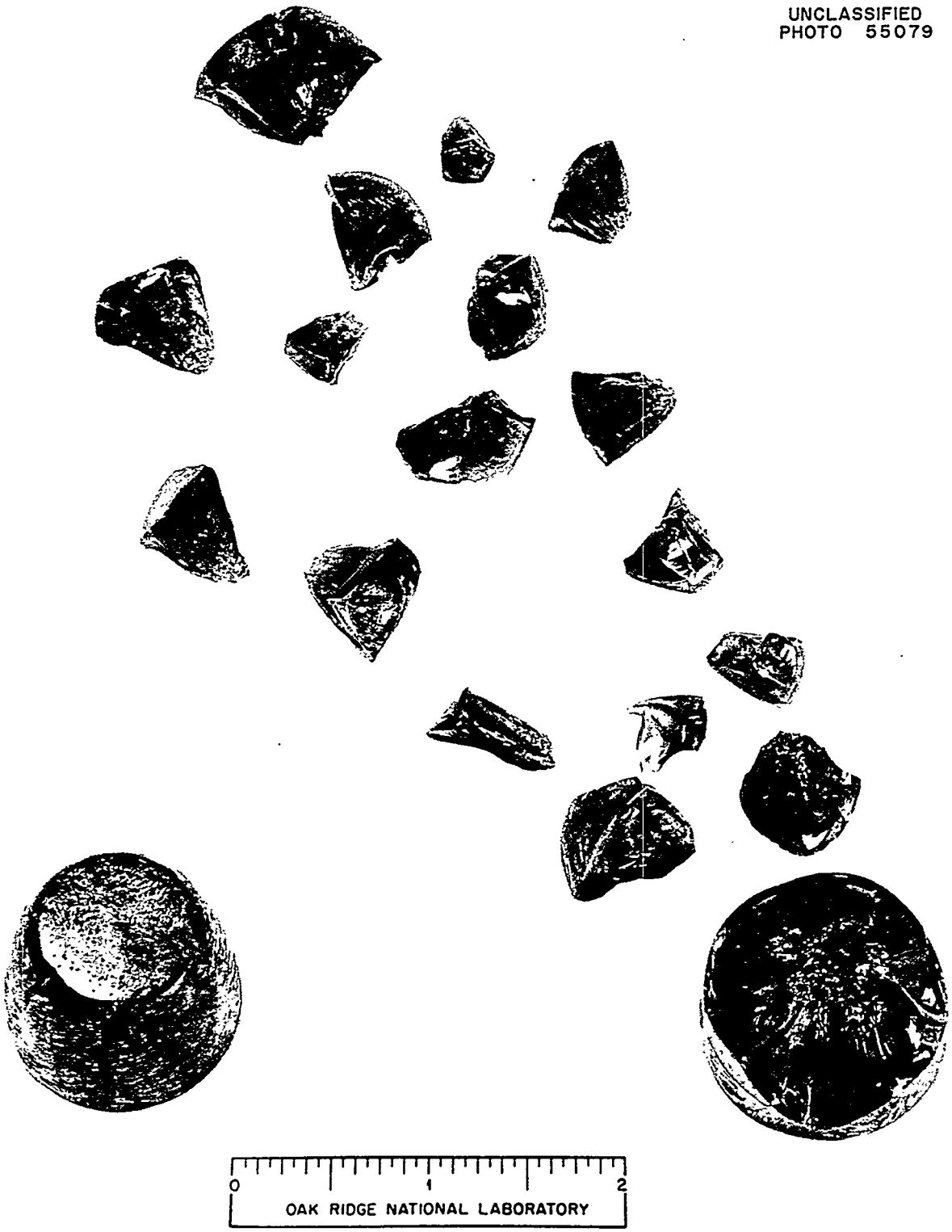

Fig. 2.1. Phosphate-Borate Glass Incorporating TBP-25 Waste Oxides. Additives (moles/liter waste): 1.52 $NaH_2PO_2 \cdot H_2O$, 0.13 $Na_2B_4O_7 \cdot 10H_2O$, 0.16 NaOH.

Table 2.4 Phosphate-Borate Glasses Incorporating Oxides from TBP-25 Wastes

Waste composition (M): 6.60 NO_3^-, 1.72 Al^{3+}, 1.26 H^+, 0.10 Na^+, 0.05 NH_4^+, 0.003 Fe^{3+}, 0.02 Hg^{2+}, 0.0003 Ru.

Melt	1	2	3	4	5
Additives (mole/liter TBP-25)					
$NaH_2PO_2.H_2O$	1.52	1.52	1.52	2.00	2.00
$Na_2B_4O_7.10H_2O$	0.13	----	0.26	----	0.13
NaOH	0.16	----	0.42	----	0.16
$NaH_2PO_4.H_2O$		0.13			
Melt composition (wt % theoretical oxides)					
Al_2O_3	31.6	33.8	28.2	29.7	26.9
Na_2O	22.9	21.0	25.5	22.1	24.0
P_2O_5	38.9	45.1	34.6	48.1	43.5
B_2O_3	6.5	----	11.6	----	5.6
Fe_2O_3	0.08	0.09	0.07	0.08	0.07
RuO_2	0.01	0.01	0.01	0.01	0.01
	99.99	100.00	99.98	99.99	100.08
Softening point (°C)	850	950	950	950	850
Bulk density (g/ml)	2.47	2.42	2.41	2.44	2.47
Waste oxides in glass (wt %)	32.9	35.2	29.3	30.9	28.0
Volume reduction (vol TBP-25/vol glass)	8.9	9.3	7.7	8.3	7.6
Appearance	Light-green glass	Greenish-white glass	Light green glass	Green glass mottled with white	Light-yellow glass

Ruthenium Volatility. The use of phosphite or hypophosphite to control ruthenium volatility is particularly attractive since these compounds are oxidized to phosphate, a fluxing agent. The results of experiments with simulated Purex waste, containing ruthenium, (Table 2.5) indicated that the amount of ruthenium volatilized depends not only on the total amount of H_3PO_3 added but also on when the H_3PO_3 is added. For example, the condensate from a batch evaporation with 0.80 mole of $H_2PO_3^-$ per liter contained 7.84% of the original ruthenium, while in a similar but semicontinuous evaporation the condensate contained only 1.31% (Expts. 9 vs 5). The volatility also seemed to depend on temperature profiles, operating rates, and other physical parameters of the system.

The results of two experiments (Expts. 7 and 9) in which all conditions and additives were the same except for the addition of 0.8 mole of hypophosphite in one and 0.8 mole of phosphite in the other indicated that hypophosphite is as good, if not better than, phosphite in controlling ruthenium volatility, 6.37 vs 7.84% Ru in the condensate. In the experiments with hypophosphite there appeared to be an exothermic reaction starting at about 80°C, which produced ~ 10 liters of noncondensable off-gas per liter of waste. This gas was absorbed later in the experiment. The one experiment with hypophosphite in stainless steel equipment gave less ruthenium in the condensate, 0.28%, than would be expected based on experiments in glass. The difference is probably explained by ruthenium plating out on stainless equipment.

The bulk of the ruthenium in the condensate in all experiments was volatilized at the higher temperatures, 150-500°C, where the nitrates in the waste begin to decompose.

The experiments were carried to about 500°C in small all-glass equipment described previously (2) or to about 1000°C in stainless steel equipment. In five experiments the waste and/or additives were added continuously to the evaporator at a rate approximately equal to the boiloff rate. In two experiments all the H_3PO_3 was added to the feed prior to evaporation, and in three, a portion was added before evaporation and the remainder at the end of the feeding period. In five other experiments waste and additives were added to the evaporator in batches. After evaporation, the material in the evaporator was heated to dryness and the residue heated to about 500°C in glass or to about 1000°C in stainless steel. Condensate samples were analyzed by gamma counting. In addition to phosphite or hypophosphite, MgO or $Ca(OH)_2$ was added to decrease sulfate volatility and $NaH_2PO_4.H_2O$ and borax were added as fluxing agents.

Nitrate-Phosphite Reaction. Previous results (2) have shown that orthophosphorous acid controls ruthenium volatility. In experiments (Table 2.6) to investigate the stoichiometry of and the influence of various cations on the reaction between nitrate and phosphite, the principal gaseous reaction product appeared to be NO. As the ratio of nitrate to phosphate was increased, increasing quantities of NO_2 were also produced. Other products were small amounts of nitrite and nitrogen and trace amounts of N_2O. Evolution of the noncondensable gases appeared to start at about 110°C, near the initial boiling point of the mixture, and to be complete by the time the boiling point of the solution had reached about 115°C.

Table 2.5 Ruthenium Volatility from Purex Waste

Waste composition (M): 6.1 NO_3^-, 5.1 H^+, 1.0 SO_4^-, 0.6 Na^+, 0.5 Fe^{3+}, 0.1 Al^{3+}, 0.01 Cr^{3+}, 0.01 Ni^{2+}, 0.002 Ru with 0.1 μc Ru-106 per ml

Expt. No.	Additive (moles/liter of waste)									Final Temp(°C)	Ru in Condensate (% of original)
	Initial H_3PO_3	H_3PO_3 after feed	NaH_2PO_2-$.H_2O$	H_3PO_2	NaH_2PO_4-$.H_2O$	$Na_2B_4O_7$-$.10\ H_2O$	NaOH	MgO	$Ca(OH)_2$		
	Continuous Feed										
1	0.05	0.35	---	---	1.12	0.13	0.46	0.80	---	500	9.41
2	0.05	0.35	---	---	1.12	0.13	0.46	0.80	---	512	12.23
3	0.05	0.35	---	---	1.12	0.13	0.46	---	0.80	440	7.77
4	0.60	---	---	---	0.92	0.13	0.67	---	0.80	493	4.03
5	0.80	---	---	---	0.72	0.13	0.87	---	0.80	493	1.31
	Batch Feed										
6	---	---	---	---	1.52	0.13	0.058	0.80	---	493	15.09
7	---	---	0.80	---	0.72	0.13	0.058	0.80	---	497	6.37
8	---	---	1.52	---	---	0.13	0.058	0.80	---	500	5.36
9	0.80	---	---	---	0.72	0.13	0.86	0.80	---	500	7.84
10*	---	---	---	1.03	0.76	0.13	0.42	---	1.00	910	0.28

*Performed in stainless steel equipment; all others in glass equipment. Total moles of P, B, and Na are constant in Expts. 1-9.

Table 2.6 Reaction of Nitrate with Phosphite

Makeup of Reaction Mixture (moles/liter)			Noncondensable Off-gases (moles)				NO_2^-	Nitrate Balance	Calc. H_3PO_3 used in Reducing NO_3^-
Expt. No.	HNO_3	H_3PO_3	N_2	N_2O	NO	NO_2	(moles)	(%)	(moles)
1	1.5	1.0	0.026	0.002	0.101	0.011	0.0027	~ 63*	~ 0.30*
2	6	1.0	0.087	0.001	0.454	0.222	0.0089	102.2	1.02
3	3	1.0	0.025	0.001	0.556	0.108	0.0449	99.6	1.06

*Since this was the first run of this series, experimental difficulties limited the accuracy of the results.

Phosphite is a strong reducing agent which reacts very slowly and in a rather complex manner with various oxidizing agents (7). The rate-determining step for the oxidation of phosphite to phosphate appeares to be the transition from an inactive, presumably $HP(O)(OH)_2$, form to an active, symmetrical form, presumably $P(OH)_3$ (8). This symmetrical form is an intermediate in the oxidation of the oxy-acids of many elements. Other investigations (9) have found the oxidation of phosphite to be catalyzed by metal cations.

Several possible reactions of nitric and orthophosphorous acids can be postulated:

$$HNO_3 + 4H_3PO_3 + H_2O \rightarrow NH_3 + 4H_3PO_4$$

$$2HNO_3 + 5H_3PO_3 \rightarrow N_2 + 5H_3PO_4 + H_2O$$

$$2HNO_3 + 4H_3PO_3 \rightarrow N_2O + 4H_3PO_4 + H_2O$$

$$2HNO_3 + 3H_3PO_3 \rightarrow 2NO + 3H_3PO_4 + H_2O$$

$$HNO_3 + H_3PO_3 \rightarrow HNO_2 + H_3PO_4$$

$$2HNO_3 + H_3PO_3 \rightarrow 2NO_2 + H_3PO_4 + H_2O$$

The nature of the reaction products depends, as is frequently the case in the reduction of nitric acid, not only on the reducing agent but also on the conditions under which the reaction is carried out.

The experiments were carried out in all-glass equipment (Fig. 2.2) with flexible polyethylene bags to collect the noncondensable off-gases. In each experiment 1 liter of the reaction mixture was placed in the reaction flask, the system was flushed thoroughly with argon, and the mixture was heated to ~ 250°C. The vapors from the flask passed through a nearly horizontal condenser to a downdraft condenser and the condensate was collected in a 200-ml flask maintained at 80-90°C. The flexible polyethylene bags, maximum capacity 2.5 liters, were connected to the system at a point between

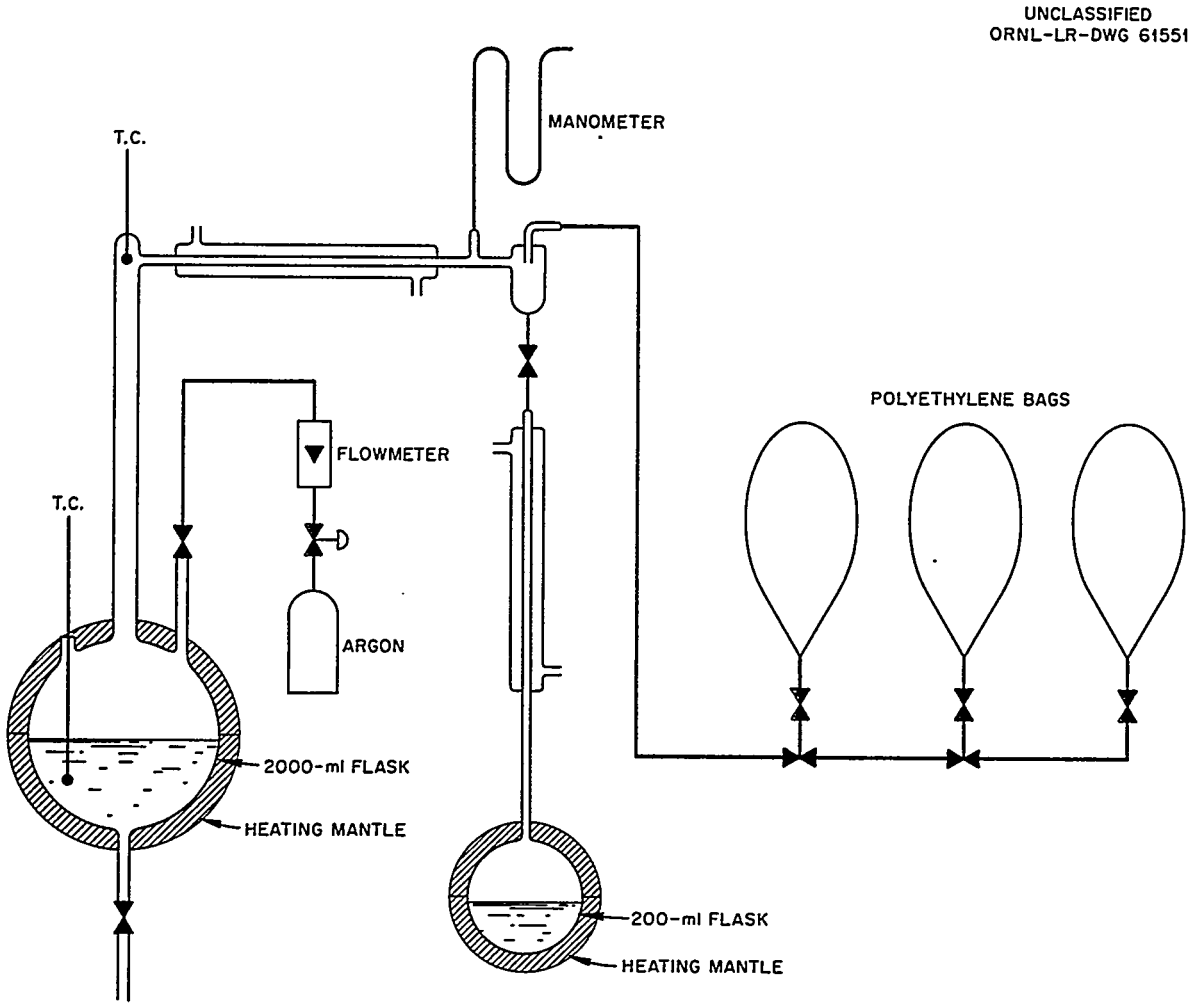

Fig. 2.2. Schematic of Apparatus for Studying HNO_3-H_3PO_3 Reaction.

the two condensers. The bags had been calibrated to give volume as a function of gas pressure. Samples of the noncondensable gases were taken in evacuated gas sampling tubes for gas chromatographic analysis for A, N_2, N_2O, NO; the amount of NO_2 was calculated by difference. Samples of the condensate and the residue were taken periodically for nitrate and nitrite determination. Samples of the residue were also analyzed for phosphate and phosphite (by determination of the reducing normality with ceric) ion. Since ceric oxidation of phosphite is also very slow, this technique probably does not give accurate phosphite values.

2.3 Design of Calcination Pilot Plant (J. O. Blomeke, J. M. Holmes)

Current plans call for installation of a demonstration waste calcination pilot plant in the ICPP radioactive pilot plant cells. The pot calciner will be demonstrated initially with TBP-25, Darex, or electrolytic dissolution, and low- and high-sulfate Purex wastes, in the order given. SIR, STR, Thorex, and Zirflex wastes will be considered for testing after the technology for their calcination is sufficiently advanced to permit design of corrosion-resistant equipment capable of containing them. Upon completion of the pot calcination program, other calciners such as the BNL rotary calciner will be tested with the same feed, off-gas contamination, and mechanical handling equipment. The use of additives to control the volatility of waste components such as sulfate and ruthenium or to form glasses from high-porosity easily leachable calcines will also be demonstrated.

Specific responsibilities for each phase of the co-operative program have been assigned. ORNL will perform the work through the laboratory, nonradioactive unit operations, and special equipment testing stages while ICPP will be responsible for the detailed engineering design, equipment installation, and radioactive pilot plant operation. A concerted effort is underway toward completing the installation of evaporation equipment at ORNL in order to provide the necessary data for radioactive pilot plant equipment design by December 1961.

Mechanical Program at Georgia Nuclear Laboratory. A contract is under negotiation with Georgia Nuclear Laboratories (Lockheed Nuclear Company) to mock up and demonstrate the remote mechanical operations required in the waste calciner pilot plant. The work will require two men, an engineer and a remote manipulator technician, for about six months and will be done in three phases:

1. Heliarc-welding of several different closure designs with nonconsumable welding rods, performed with a fixed electrode and rotating part, will be tested. Welds will be inspected by radiographing or sectioning. Pressure tests at operating temperature will be made on the final welded closures and their integrity established by helium leak-testing.

2. Mechanical equipment for remote operation will be demonstrated. Positioning of the pot calciner and furnace, connecting of the calciner pot to its vapor line, removal of the pot from its connector, and closure of the pot will be carried out. A series of tests at operating temperature (400°C) will be made on a gasketed joint designed by ORNL and a Grayloc seal, which will be helium leak-tested. Sealing of the pots with either a gasketed closure or Grayloc joint will also be demonstrated and leak-tested.

3. If the welded closure tests are successful, a remote welding machine will be purchased and demonstrated.

3.0 LOW-LEVEL WASTE TREATMENT

A scavenging-ion exchange process (10-13) is being developed for decontaminating the large volumes of slightly contaminated water produced in nuclear installations; ORNL low-activity-level waste is being used as a medium for study. The scavenging-ion exchange process uses phenolic resins, as opposed to polystyrene resins, since the phenolic resins are much more selective for cesium in the presence of sodium; the Cs/Na separation factor is 160 for CS-100 or C-3 resin vs 1.5 for Dowex 50 resin. Other cations, e.g., strontium and rare earths, are also sorbed efficiently. Inorganic ion exchange media such as vermiculite and clinoptilolite are being studied as alternatives. The waste solution must be clarified prior to ion exchange since ion exchange media do not remove colloidal materials efficiently. Water clarification techniques are being developed for both the ion exchange processes and for the ORNL lime-soda process waste water treatment plant. Work is proceeding on both development and pilot plant programs.

3.1 Scavenging-Ion Exchange Processes

Demonstration Run (W. E. Clark, R. R. Holcomb). A third demonstration of the phenolic ion exchange process was completed in the 60-liters/hr semi-pilot plant facility (Figs. 3.1 and 3.2) in the basement of the ORNL low-activity-level-liquid-waste treatment plant. At 1500-1600 bed volumes only the Cs-137 effluent activity exceed the 1% breakthrough level; the other activities were still being effectively removed from solution (Table 3.1). The necessary d.f.'s, > 1000 for Sr, 100 for TRE, and > 100 for Cs, were achieved prior to 1500 bed volumes of waste treated, thus guaranteeing discharge at less than 10% of the mpc.

The run consisted in pumping process water waste at a rate of 1 liter/min into a 0.3-min hold-up flash mixer, along with 19 M NaOH and copperas ($FeSO_4.7H_2O$) coagulants to maintain a pH of 11.7 and an ion concentration of 5 ppm, respectively. After a 45-min flocculation and a 3-hr sludge-blanket clarification, the water was filtered through an anthracite coal column to remove the last traces of solids, then through a compacted cellulose-fiber filter to determine the effectiveness of the coal filter, finally treated with a carboxylic-phenolic cation exchange resin, Duolite CS-100, to remove the remaining soluble activities.

A comprehensive topical report, covering the development of this process from batch laboratory studies to pilot plant scale, is being prepared.

Design of Pilot Plant (J. O. Blomeke, J. M. Holmes, W. R. Whitson). A pilot plant is being installed for demonstration of the cleanup of ORNL process waste by scavenging and ion exchange. Details of the process flowsheet were given in reference (2), pp. 37-41.

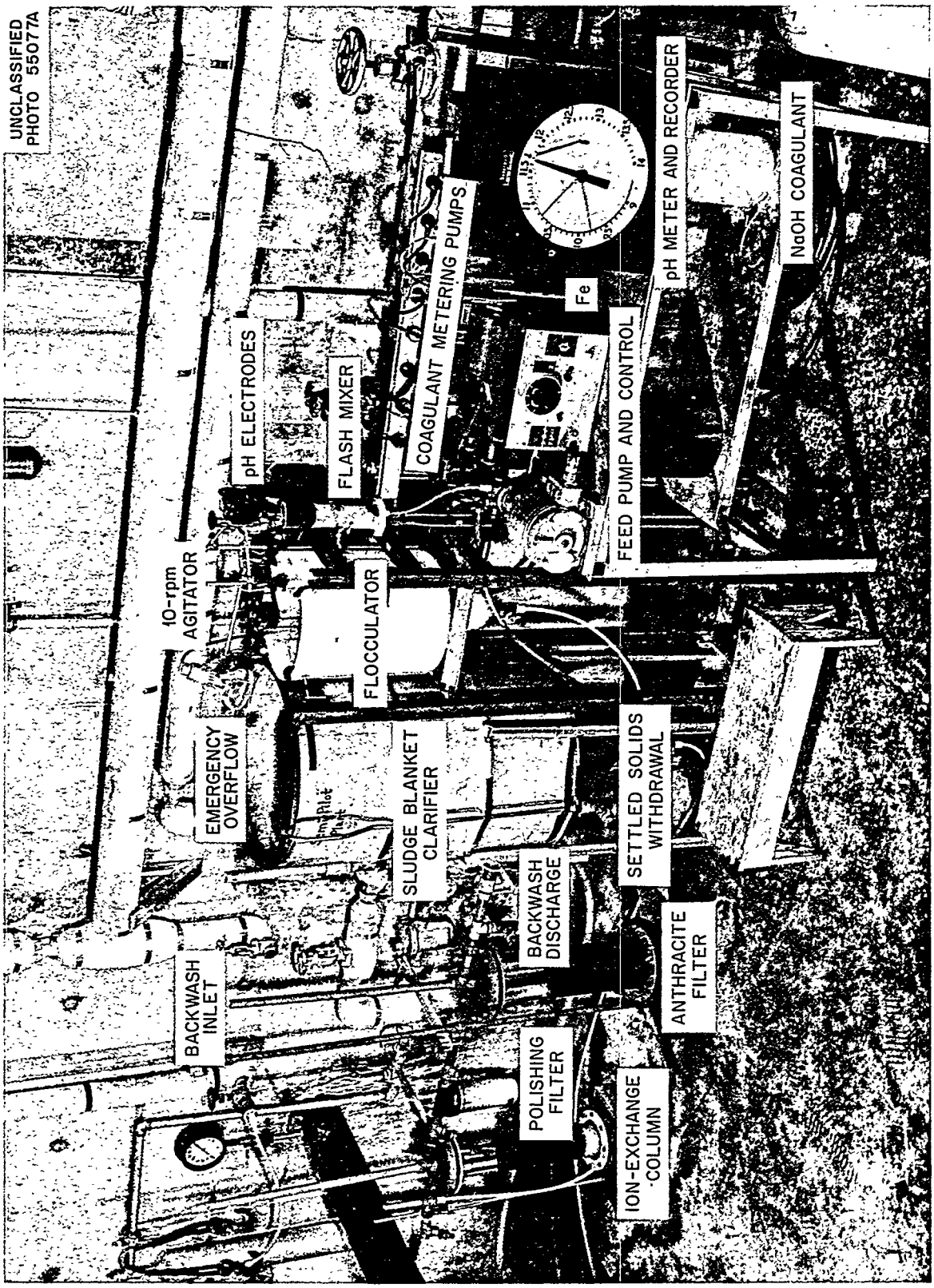

Fig. 3.1. Semi-Pilot Plant for Demonstration of Ion Exchange Treatment of Low-Level Process Waste Water.

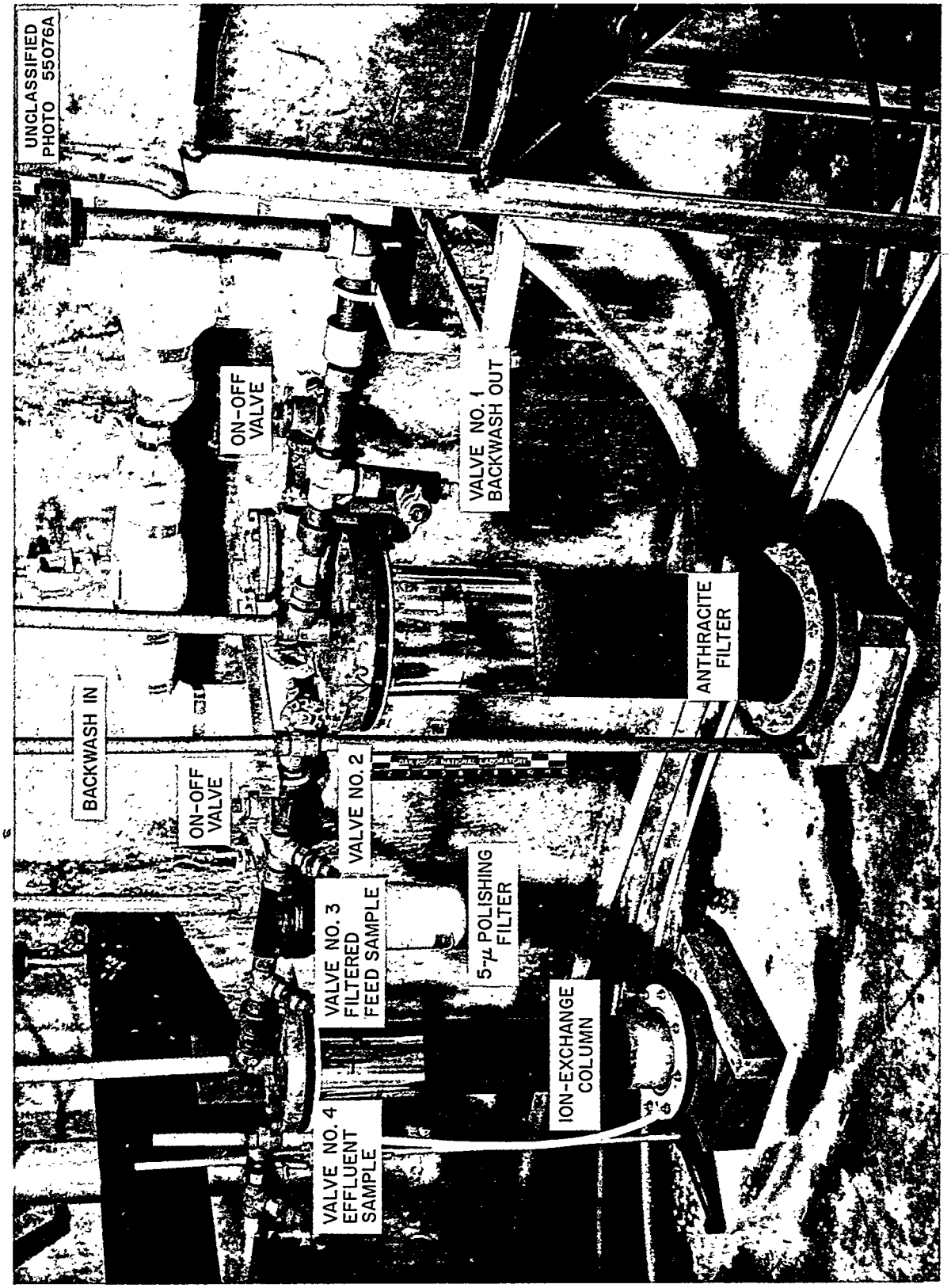

Fig. 3.2. Filtration and Ion Exchange Portion of Semi-Pilot Plant Unit.

Table 3.1 Decontamination of ORNL Low-Level Waste by the Scavenging-Ion Exchange Process; 60 liters/hr Pilot Plant Tests

	Solution Activity ($d\ min^{-1}\ ml^{-1}$)								
	Radiochemical			Gamma Spectrometry					
Code	Gr-β	TRE-β	Sr-β	Ru-106	Cs-137	Co-60	Zr-Nb-95	Zn-65	Sb-125
SPP Run 3									
1156 bed volume									
Feed	462	129	110	3.10	19.44	8.53	9.81	2.78	1.55
Effluent	99	1.98	0.04	3.73	0.09	3.70	0.60	< 1	n.d.
1587 bed vol									
Feed	460	---	123.2	6.24	22.14	6.74	---	trace	8.64
Filtered Feed	146	---	36.43	5.67	15.5	3.16	---	n.d.	9.08
Effluent	61	---	0.07	1.97	0.24	2.94	---	n.d.	4.82
1876 bed vol									
Feed	440	199	122	5.47	29.0	7.49	13.1	1.40	4.48
Effluent	26	1.58	0.05	1.65	0.74	1.46	trace	n.d.	2.54

n.d. = not detected

Consideration of the handling problems created by removal of radioactive sludge from the plate-and-frame filter originally proposed led to installation of two vertical granular-bed pressure filters. However, the plate-and-frame filter will be used in the initial, nonradioactive, tests to determine the filtration characteristics of the sludge produced by the clarifier in pressure filtration with precoat and filter aid. Vacuum filtration tests will also be conducted on this sludge. The vertical bed filters are plastic-lined, 2-ft-dia by 4-ft-straight section, vessels with bottom liquid distributor. An anthracite bed 2-3 ft deep will be tested in one filter and a sand bed of the same depth in the other. Process water for backwashing the filters periodically will be stored and recycled to the feed stream in order to confine all solids to the clarifier sludge stream. Current tests on a small, 1-liter/min, anthracite filter bed indicate that backwashing will probably not be required more frequently than every three days, which will be the duration of a test run.

Pilot plant tests on ORNL tap water (no radioactivity) will probably start by September 1, 1961. These tests will include demonstration of the flash mixer, flocculator, clarifier, and sludge filtration equipment. After completion of the 2-in.dia process water feed pipeline from the basement of the lime-soda treatment plant to the pilot plant, the tests will be extended to the ion exchange equipment with slightly contaminated process water. This pipeline should be completed by Oct. 1, 1961.

3.2 Inorganic Ion Exchange of Process Waste Water Treatment Plant Effluent (K. E. Cowser)

Natural Minerals for Second stage Treatment. A number of natural minerals (Table 3.2) were tested for their ability to remove Sr-90 and Cs-137 from the Process Waste Water Treatment Plant effluent (12). Particle size was an important parameter in the use of natural minerals, the smaller particles being the most efficient.

Physical breakdown of a mineral on contact with water would make it unsuitable for use in columns. In all tests on resistance to the flow of water in small laboratory columns, or 2 in. dia and containing 18 in. of mineral, the head loss through the column varied linearly with the flow rate. Under the test conditions all the materials tested were acceptable.

The physical characteristics of vermiculite are likely to change as a result of bed compaction or chemical treatment. A 2-in.-dia x 12-ft-high glass column was charged with 9 ft of vermiculite (BO-4 grade), and the loss of head determined with fluid typical of process waste. The resistance to flow during upflow operation agreed with results obtained in a 1.5-ft-high column; channeling began at a flow rate of 2.5 ml min^{-1} cm^{-2}. However, during downflow operation, the head loss (37.5 cm of water per foot at 4 ml min^{-1} cm^{-2}) was twice that in the shorter column. After the vermiculite was treated with NaCl (80 liters of 12% solution) and NaOH (35 liters of 0.2 M solution),

Table 3.2 Physical Characteristics of Natural Minerals

	Particle Size			Loss of Head (cm H_2O/ft bed depth)	
	Effective Size (mm)	10% and 90% Passing Size (mm)	Uniformity Coefficient	Flow Rate of 0.5 gal min^{-1} ft^{-2}	Flow Rate of 1.0 gal min^{-1} ft^{-2}
Vermiculite BO-1	2.1	2.1 - 3.8	1.3	0.75	1.5
Vermiculite BO-2	2.0	2.0 - 2.6	1.1	1.1	2.2
Vermiculite BO-3	0.41	0.41 - 1.6	2.4	5.0	11.0
Vermiculite BO-4	0.17	0.17 - 0.49	2.3	10	20
Rock phosphate					
Fine	0.25	0.25 - 0.80	1.9	16	32
Coarse	1.1	1.1 - 4.0	2.8	1.5	3.0
Clinoptilolite	---	0.21 - 0.50*	---	---	---

*Size range represents lower and upper limit of the clinoptilolite studied.

the head loss increased to 120 cm H_2O per foot at 2 ml min^{-1} cm^{-2}, primarily because of breakdown of the vermiculite by the caustic treatment. Although head loss was decreased by backwashing to remove the excess fine material, full recovery did not occur; the loss remained 1.6 times that before treatment. Since mechanically cleaned vermiculite does not require caustic treatment, its use should obviate this difficulty.

Vermiculite Column Pilot Plant. Design of a 3-gal/min pilot plant to demonstrate the effectiveness of sodium-treated vermiculite ore (BO-4 grade) for second-stage treatment of ORNL process waste was completed and construction is underway. Effluent from the Process Waste Water Treatment Plant will be pumped to the pilot plant (Fig. 3.3), which will contain a 3-gal/min Viking pump with variable-speed drive, chlorine supply tank and 200-ml/min Milton Roy Mini-pump, an 8-gal/min Cuno (model IB2) filter, a vermiculite column with 12 in. dia x 10 ft high bed, flow-rate meter, integrating water meter, continuous beta-gamma monitor, and recording pH meter.

The initial run will test vermiculite ore, but other natural minerals that have shown promise in the laboratory may be tested with the same equipment. Chlorination of the waste is necessary to prevent eventual plugging of the column by biological growths. The principal purpose of the Cuno filter is to clarify the influent to the column and not to obtain design data on its suitability for large-scale operation. A backwash and surface spray system is included with the column in the event that excessive resistance to flow develops in the vermiculite bed. Provision is made for sampling the vermiculite bed after use and for its disposal as a contaminated solid in Burial Ground 5.

4.0 ENGINEERING, ECONOMIC, AND HAZARDS EVALUATION

J. O. Blomeke, R. L. Bradshaw, J. J. Perona, and J. T. Roberts

A comprehensive study has been undertaken to evaluate the economics and hazards associated with alternative methods for ultimate disposal of highly radioactive liquid and solid wastes. All steps between fuel processing and ultimate storage will be considered, and the study should define an optimum combination of operations for each disposal method and indicate the most promising methods for experimental study.

A 6-tonne/day fuel processing plant is assumed, processing 1500 tonnes/year of uranium converter fuel at a burnup of 10,000 Mwd/tonne and 270 tonnes/year of thorium converter fuel at a burnup of 20,000 Mwd/tonne. This hypothetical plant would process all the fuel from a 15,000-Mw_e nuclear economy, which may be in existence by 1970. The preliminary operations to be evaluated are interim liquid storage, conversion to solids by pot calcination, interim storage of solids in pots, and shipment as either liquids or calcined solids. The ultimate disposal methods to be evaluated are calcined solids in salt deposits, in vaults, and in vertical shafts and liquids in salt deposits, in deep wells, by hydrofracture, and in tanks.

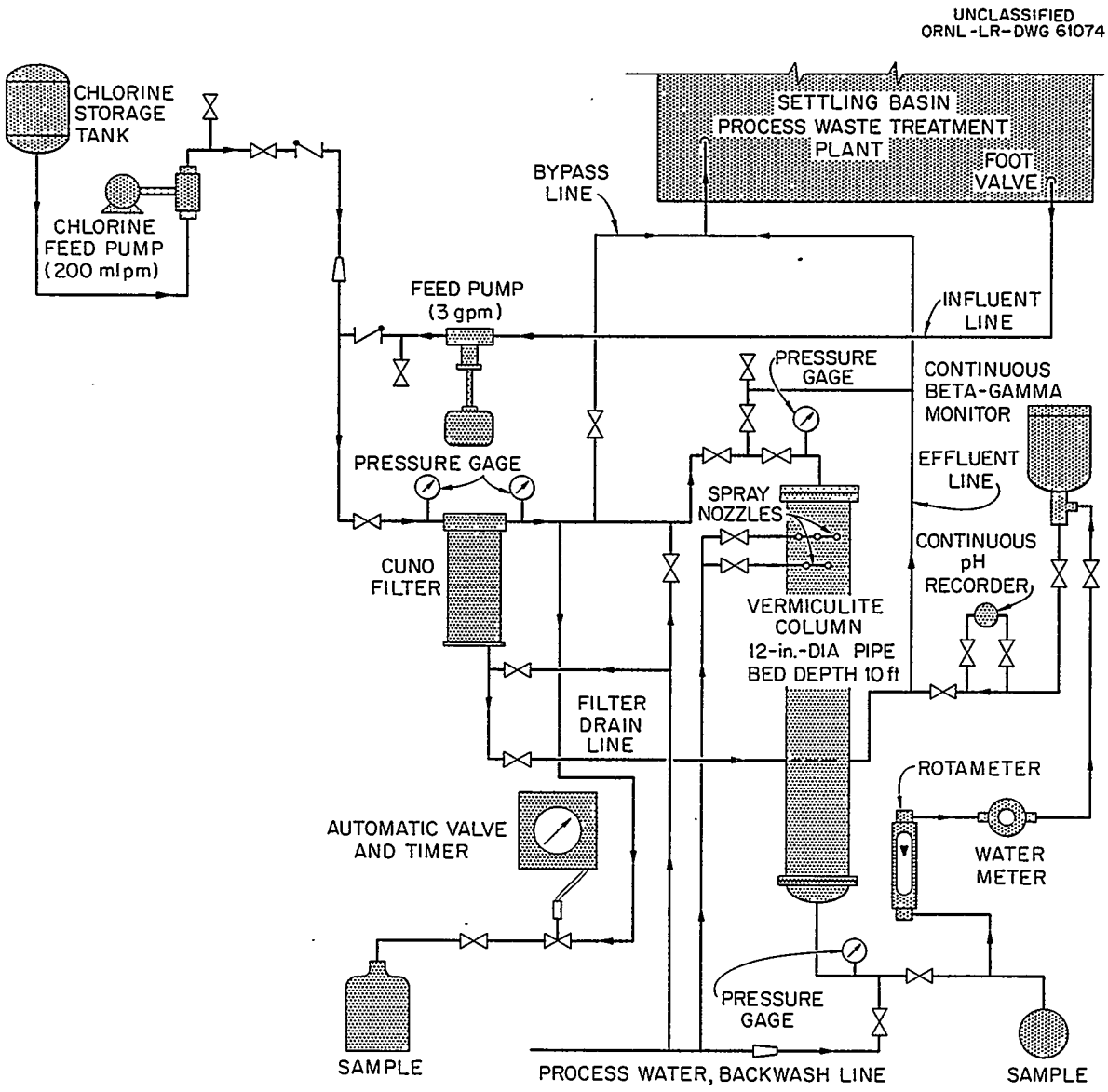

Fig. 3.3. Preliminary Flowsheet for Low-Level Waste Vermiculite Column in Pilot Plant.

4.1 Cost of Pot Calcination of High-activity Waste

A cost study of conversion of high-activity solutions to solid by pot calcination was completed (14). Costs were calculated for processing Purex and Thorex wastes in acidic and reacidified (after alkaline storage) forms and for producing Thorex glass from acidic wastes. Calcination vessel designs were right circular cylinders similar to those used in engineering development studies. The vessels chosen for study were 6, 12, and 24 in. dia, made of schedule 40 type 347 stainless steel pipe, 10 ft high. Vessel costs used, based on estimates from private industry, were $500, $855, and $2515, respectively. Costs were calculated for wastes decayed 120 days and 1, 3, 10, and 30 years after reactor discharge prior to calcination. Aging had negligible effect on costs for processing in a given vessel size, because vessel and operating costs were much higher than capital costs in all cases. Aging permits larger vessels to be used, however, and costs for processing in 6-in.-dia vessles were 2 to 3 times as high as for processing in 24-in.-dia vessels.

The lowest cost was 0.87×10^{-2} mill/kwh$_e$ for processing acid Purex and Thorex wastes in 24-in.-dia vessels, and the highest was 5.0×10^{-2} mill/kwh$_e$ for processing reacidified Purex and Thorex wastes in 6-in.-dia vessels. (Table 4.1). About 7 yr of interim liquid storage would be required before acidic Purex waste could be processed in 24-in.-dia vessels.

Table 4.1 Pot Calcination Costs as Affected by Wastes Types and Vessle Sizes

Waste Type	Total Processing Cost (mills/kwh$_e$)		
	6-in.-dia Vessels	12-in.-dia Vessels	24-in.-dia Vessels
Acidic Purex-acidic Thorex	1.6×10^{-2}	0.98×10^{-2}	0.87×10^{-2}
Acidic Purex-acidix Thorex glass	2.2	---	---
Acidic Purex-reacidified Thorex	3.8	1.9	1.5
Reacidified Purex-acidic Thorex	2.8	1.5	1.2
Reacidified Purex-acidic Thorex glass	3.4	---	---
Reacidified Purex-reacidified Thorex	5.0	2.4	1.9

4.2 Storage of Processed Waste

The step in the economic study of ultimate disposal methods currently under study is ultimate disposal of liquid and solid wastes in salt mines. In cost figures to be developed, the amount of mine space required to safely dissipate the fission product heat produced by wastes of different types and ages must be specified.

For liquid wastes it is assumed that disposal will be in rooms with recessed floors filled with granular salt. If rooms are relatively large, e.g., 50 by 100 ft, peak waste temperatures in the center of a room will not be too different from that in a layer with infinite horizontal dimensions. A computer code is available for obtaining the temperature rise in an infinite slab with a decaying heat source (see Sect. 6.0). The graph in that section shows peak slab temperature rise as a function of decay time for 1 gal/ft^2 (of slab) of waste whose heat generation 120 days after reactor discharge is 100 watts/gal. Since wastes assumed in this study have a somewhat different heat decay scheme, an additional computation was made which resulted in a similar curve. It is felt that this calculation will be adequate for assessing space requirements for disposal of liquids in salt.

The solid wastes to be disposed of are pot-calcination cylinders 6, 12, or 24 in. dia by 10 ft high. For purposes of personnel shielding during operation, it will be advantageous to store the cylinders in holes in the floor. Under these conditions the slab calculations will determine the average salt temperature rise, but to get the perturbations produced by the cylinders another approach is necessary. If the cylinders are equally spaced on triangular centers, each will be in the middle of a hexagonal area which is peculiar to itself. If there are a large number of cylinders, all containing identical heat sources and all placed in the mine simultaneously, it may be assumed that no heat flows across the vertical boundaries of the hexagonal area. If the hexagonal boundary is approximated by a circle, the problem reduces to that of a single finite-length cylindrical heat source in the center of an infinitely long cylinder whose sides are perfectly insulated. For temperatures outside the heat generating cylinder an insignificant error will be introduced if the heat source is assumed to be a line in the center of the cylinder.

An equation for the temperature rise in an infinitely long cylinder due to an instantaneous point source of heat is given by Carslaw and Jaeger (15). This equation was integrated on the axial dimension to obtain an expression for an instantaneous line source. Since the heat generation rate used in this study is the sum of eight decaying exponentials, the solution for the case of exponential heat generation decay was obtained from the solution for the instantaneous line source by a superposition or convolution integral. The resulting equation is

$$V = \sum_{i=1}^{m} \frac{Q_i}{\pi\rho c a^2} e^{-\lambda_i t} \left\{ \frac{2}{\lambda_i} \left[e^{\lambda_i t} \operatorname{erf} \frac{b}{\sqrt{4kt}} - 1 + e^{(\lambda_i t - b^2/4kt)} \operatorname{Rw}\left(\sqrt{\lambda_i t} + \frac{ib}{\sqrt{4kt}} \right) \right] \right.$$

$$+ \sum_{n=1}^{\infty} \frac{J_o(\alpha_n r)}{(\lambda_i - k\alpha_n^2)\, J_o^2(\alpha_n a)} \left[e^{(\lambda_i - k\alpha_n^2)t} \operatorname{erf} \frac{b}{\sqrt{4kt}} - 1 + \cosh\left(b \sqrt{\frac{|\lambda_i - k\alpha_n^2|}{k}} \right) \right.$$

$$\left. \left. + \frac{1}{2} e^{-b\sqrt{\frac{|\lambda_i - k\alpha_n^2|}{k}}} \operatorname{erf}\left(\sqrt{|\lambda_i - k\alpha_n^2|\, t} - \frac{b}{\sqrt{4kt}} \right) - \frac{1}{2} e^{b\sqrt{\frac{|\lambda_i - k\alpha_n^2|}{k}}} \operatorname{erf}\left(\sqrt{|\lambda_i - k\alpha_n^2|\, t} + \frac{b}{\sqrt{4kt}} \right) \right] \right\}$$

Where V = temperature rise in infinite cylinder at a radial distance r from the center of the continuous line source, ^{o}F

Q_i = heat generation of i-th nuclide at time of burial of waste, Btu/hr.ft

ρc = volume heat capacity of medium, Btu ft^{-3} $^{o}F^{-1}$

a = radius of infinite cylinder, ft

λ_i = decay constant of i-th nuclide, hr^{-1}

t = time after burial of waste, hr

$2b$ = length of line source, ft

k = thermal diffusivity of medium, ft^2/hr

$Rw(z)$ = real part of complex error function $w(z)$, dimensionless

$i = \sqrt{-1}$

$\alpha_n a$ = positive roots of $J_1(\alpha a)$, excluding $\alpha_n = 0$

r = radial distance from center of infinite cylinder, ft

Temperatures were calculated in a 10-ft-dia infinite cylinder for two values of r at t = 6 hr, requiring 41 terms in the series on α to get adequate convergence. At 6 hr the temperature at the wall of the cylinder was not yet affected by the line source, and the results were checked by the simpler expression for a finite line source in an infinite solid medium. The equation for the finite line source in the infinite cylinder is now being programmed for the IBM 7090 computer.

5.0 DISPOSAL IN DEEP WELLS

5.1 Disposal by Hydraulic Fracturing (W. de Laguna)

Test drilling at the site of the second fracturing experiment is nearly completed. The upper grout sheet is now known to extend out from the injection well some 500 ft to the east and northeast, but only short distances in other directions. This sheet is composed of four separate layers, formed one above the other. The lower grout sheet extends largely to the north and northwest but its outer limits are still undefined. Locally, at least, it also is composed of more than one sheet. A detailed analysis of the geologic structure, which appears to have determined the directions in which the grout sheets moved, will have to wait until the deviation from vertical of the test holes has been measured, for with holes 800 to 1000 ft deep even a slight bend is significant.

The deep test well at the proposed site of the Waste Disposal Fracturing Plant is now at ~ 2200 ft of a proposed total depth of 3500 ft. Rock well-suited to disposal operations has been encountered from 1500 ft to the present bottom of the hole, with more in prospect.

6.0 DISPOSAL IN NATURAL SALT FORMATIONS

6.1 Field Tests (F. M. Empson)

After removal of the waste from the experimental cavities, changes in the cavity walls were noted by photographs, by weighing the redeposited salt, and by direct measurements. Changes in the cavity walls are shown most graphically in the photographs (Figs. 6.1-6.3). Determination of the weight of material dissolved and redeposited gives an average value for the enlargement of the cavity, but does not give any indication of variations in dissolution from one area to another. Measurements show changes from the original dimensions and indicate the location of pockets and areas of salt buildup on the walls. This information should make possible computation of the final volume of dissolved salt and making of a material balance on the movement of salt.

Acid Cavity. After removal of recrystallized salt from the walls and bottom of the acid waste cavity, the upper 12 in. of wall, which had been protected by the off-gas cover and the seal trench, were seen to be unchanged. The pure salt, 12-18 in. down from the floor, was undercut 1-2 in. From 18 to ~ 24 in., there was closely bedded shale and salt from which the salt had been partially dissolved. Below this, and continuing on down to the liquid level, there was a reticulated area of anhydrite and/or shale from which the salt had been dissolved. From the liquid level at 2.5 to ~ 9 ft below the mine floor, the wall was partially covered with recrystallized salt. Localized dissolution resulted in pitting to depths of 8-9 in., particularly in the upper half of this zone. On the other hand, very little shale had been displaced from the walls, but it was weak and spongy as a result of chemical attack by the waste.

The bottom of the cavity was covered by a thick layer of dense recrystallized salt, varying in thickness from as much as 16 in. at the wall to ~ 4 in. near the center. When this material was chipped away, the original cavity wall and floor were found to be unchanged.

Petrographic analyses are being made of the crystalline salts and acid-affected shale found in the cavity.

Approximately 7400 lb of material (recrystallized salt and some shale) was chipped from the walls and floor of the acid pit. If this is considered to have come from the walls, it represents an average penetration of 1.9 in. If the unattacked area at the bottom of the cavity is not included in the calculation, the average penetration is 2.5 in.

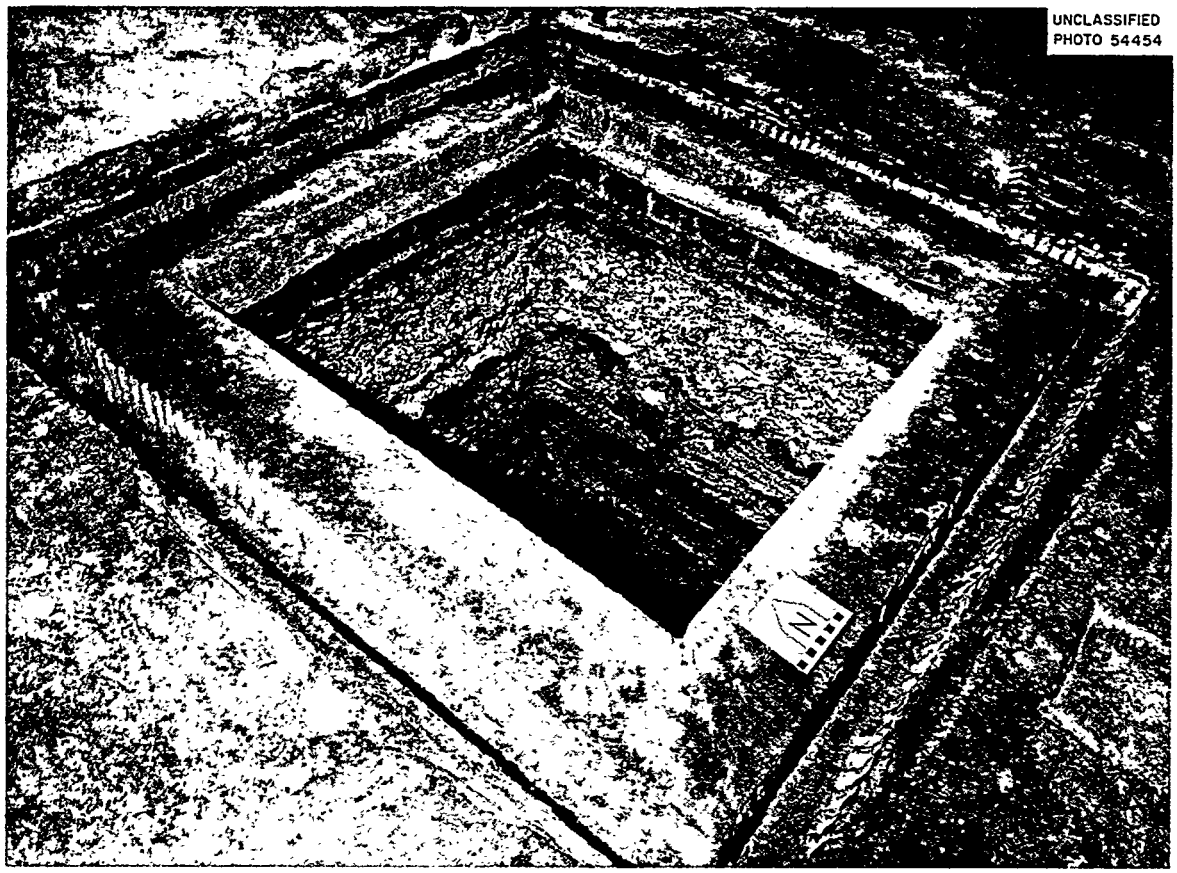

Fig. 6.1. Acid Waste Cavity, from the Top, After Removal of Recrystallized Salt.

Fig. 6.2. Interior of Neutralized Cavity Before Cover Removal.

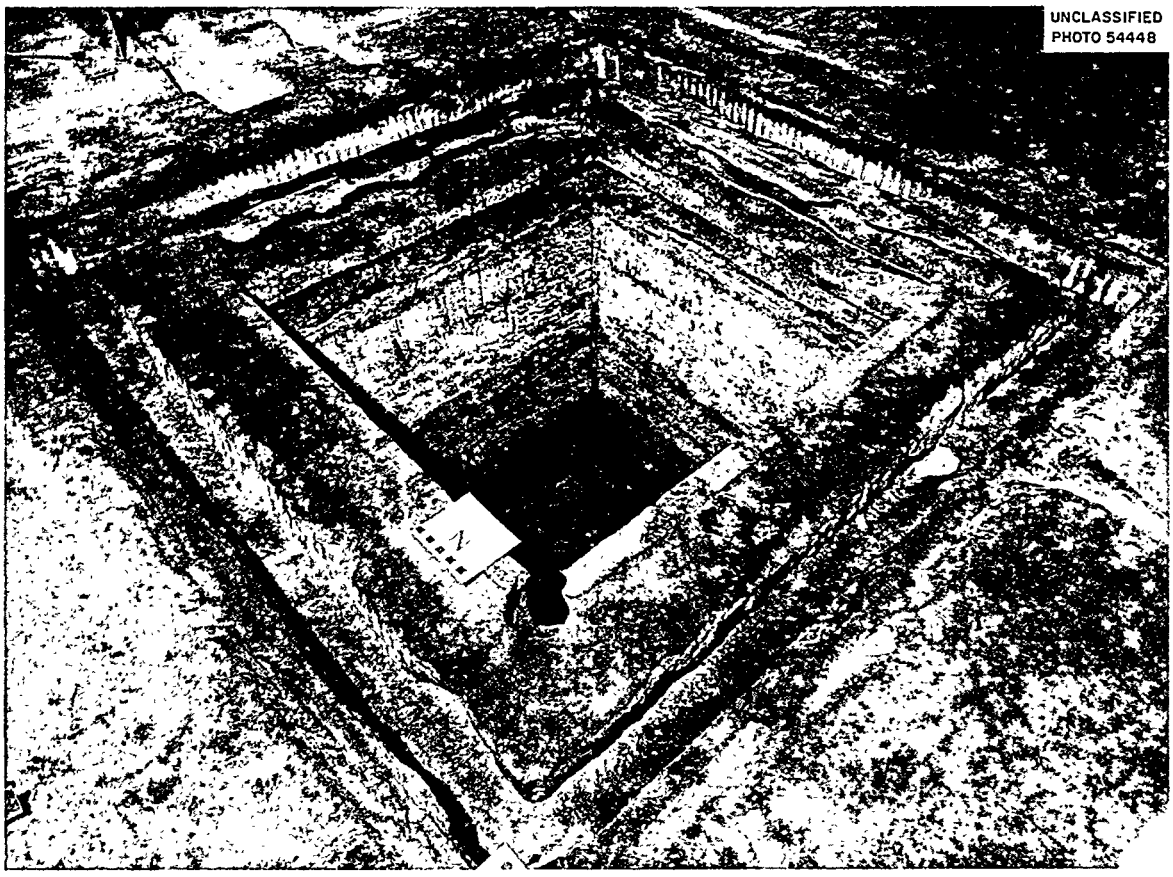

Fig. 6.3. Neutralized Waste Cavity After Removal of Recrystallized Salt.

Neutralized Cavity. In the neutralized waste cavity, before removal of cover and electrodes, a large amount of recrystallized salt bridging out from the wall to the electrodes was seen, as well as deposits on the walls below the bridge and over the sludge layer in the bottom of the cavity (Fig. 6.2). From the top of the cavity, after removal of the cover and recrystallized salt from the side walls, the deep erosion of the wall just below the rim of the cavity could be seen (Fig. 6.2). An anhydrite band, beginning about 10 in. below the floor, was undisturbed. Below the anhydrite band (15-21 in. down) salt mixed with shale was eroded to maximum depths of 15-18 in. Recrystallized salt bridged out from 21 in. down to the liquid level elevation (30 in. down). Below this the wall was covered by 1-2 in. of crystalline salt down to the precipitate, occupying 24-30 in. at the bottom. It is obvious that the condensate collection system was less effective in preventing erosion of the upper part of the cavity than was the system on the acid cavity. Minor differences in the cover and off-gas system may be responsible for this, although the installations were supposedly identical. Support is lent to this hypothesis by the fact that condensate collection, at peak waste temperature, from the neutralized cavity averaged about 0.5 gal/day, while condensate collection from the acid cavity was 1.5 gal/day.

It was not possible to obtain an accurate figure for the amount of recrystallized salt deposited in the neutral cavity, as there was a considerable amount of salt in the sludge which could not be separated. After removal of the waste, ~ 5600 lb of salt was chipped from the walls. If this was removed evenly from the upper 2 ft of the walls, the depth of erosion would be about 8 in.

6.2 Plastic Flow Studies (W. J. Boegly, Jr.)

In order to determine more accurately the effect of temperature on the rate of plastic flow, a series of small experiments, called "heated rooms," are planned. These rooms, approximately 2 ft high by 6 ft wide by 8 ft deep, will be excavated in selected pillars of the Carey Mine in Hutchinson, Kansas. Immediately after the excavation the overburden pressure will be measured, and gages will be installed to measure the plastic flow at ambient temperature. The rooms will then be heated and the increase in flow measured under various combinations of temperature and stress.

Linear displacement transducers, capable of operation at temperatures up to 200°C, have been purchased, and a mockup is being prepared to test all components prior to field installation. The transducers will be installed so that measurements can be made of movement in the floor and ceiling and between the walls. Thermocouples installed in the salt surrounding the room will be used to obtain the temperature profiles needed to correct for thermal expansion.

To obtain additional plastic flow measurements at ambient temperature, three gages have been installed in the Carey Salt Company's Lyons Mine to measure the flow at greater depth (1000 ft in Lyons vs 650 ft in Hutchinson) in rooms of various sizes. These data will be correlated with the measurements in the Hutchinson mine to determine the effect of increased overburden pressure. Stress measurements will be made in the salt near each gage.

Stress measurements were made in the floor and in three pillars of the Carey Salt Mine in Hutchinson (Fig. 6.4) (made for ORNL by the Bureau of Mines) with borehole deformation gages in the salt. Changes in borehole deformation were measured in both the horizontal and vertical directions so that stresses in the two directions could be determined. The measurements indicate no horizontal stress in the mine pillars; the vertical stress (1300-1600 psi) is less than expected on the bases of overburden pressure and percentage extraction (1950 psi).

6.3 Thermal Studies (R. L. Bradshaw)

Analysis of Large-scale Field Data. The theoretical time-space temperature rise about a sphere with constant heat generation can be normalized so that the temperature rise in relation to heat generation rate, sphere radius, and thermal conductivity of the medium can be plotted against time in relation to sphere radius and thermal diffusivity of the medium (Fig. 6.5). The family of curves thus obtained applies for distances from the sphere in terms of sphere radii. When plotted on log graph paper, the thermal conductivity and diffusivity of the infinite medium can be determined by superimposing experimental time-space temperature rises obtained about spheres. In the case of a 7.5-ft cube of neutralized waste, the localized heating in the precipitate phase makes such a comparison invalid. The acid-waste cavity (Fig. 6.6), however, gives a reasonably good check if the comparison is confined to portions of the curves that represent a temperature rise greater than 1°C and time less than 20 days after startup. (The accuracy of the temperature recordings is approximately ± 0.5°C, and after 20 days the heat loss through the floor becomes appreciable.) When the acid-waste cavity wall temperature is matched with the theoretical curve for r = a (Fig. 6.5), the 2.5-, 4-, and 8-ft-out curves (Fig. 6.6) agree closely with the r = 1.5a, 1.8a, and 2.6a curves, respectively, that is, with the theoretical curves for a 5-ft-radius sphere. The 0.5-ft-out curve does not agree so well, perhaps due to an inaccurately placed thermocouple. From this comparison, the calculated thermal conductivity is 2.6 Btu hr^{-1} ft^{-1} $°F^{-1}$, and the diffusivity 0.099 ft^2/hr, which corresponds to the Birch values (16) for single pure-salt crystals at 80 and 65°C, respectively. The peak salt temperature over the portions of the curves compared was from 25 to 60°C, perhaps indicating that the bedded Kansas salt is a somewhat poorer heat conductor than pure salt crystals.

An equation was derived from which the variation (due to electrode resistance) of power input with depth in the 7.5-ft waste cube could be calculated (Fig. 6.7). The initial power input to the cavity was 5.8 kw. For comparison purposes, data on a 10-in. laboratory block experiment are also shown. The vertical temperature-rise profile in the 7.5-ft-cube acid-waste cavity (Fig. 6.7) indicates that convection currents set up by the localized heating immediately around the electrodes tended to equalize the temperature throughout the cavity. The bottom foot or so seems to be much cooler than the rest, and is apparently explained by the fact that the thermocouples located at points 3 in. and 1 ft off the bottom of the cavity were actually in redeposited salt. In the top 6 ft of solution there was only a degree or so variation in either the horizontal or vertical direction.

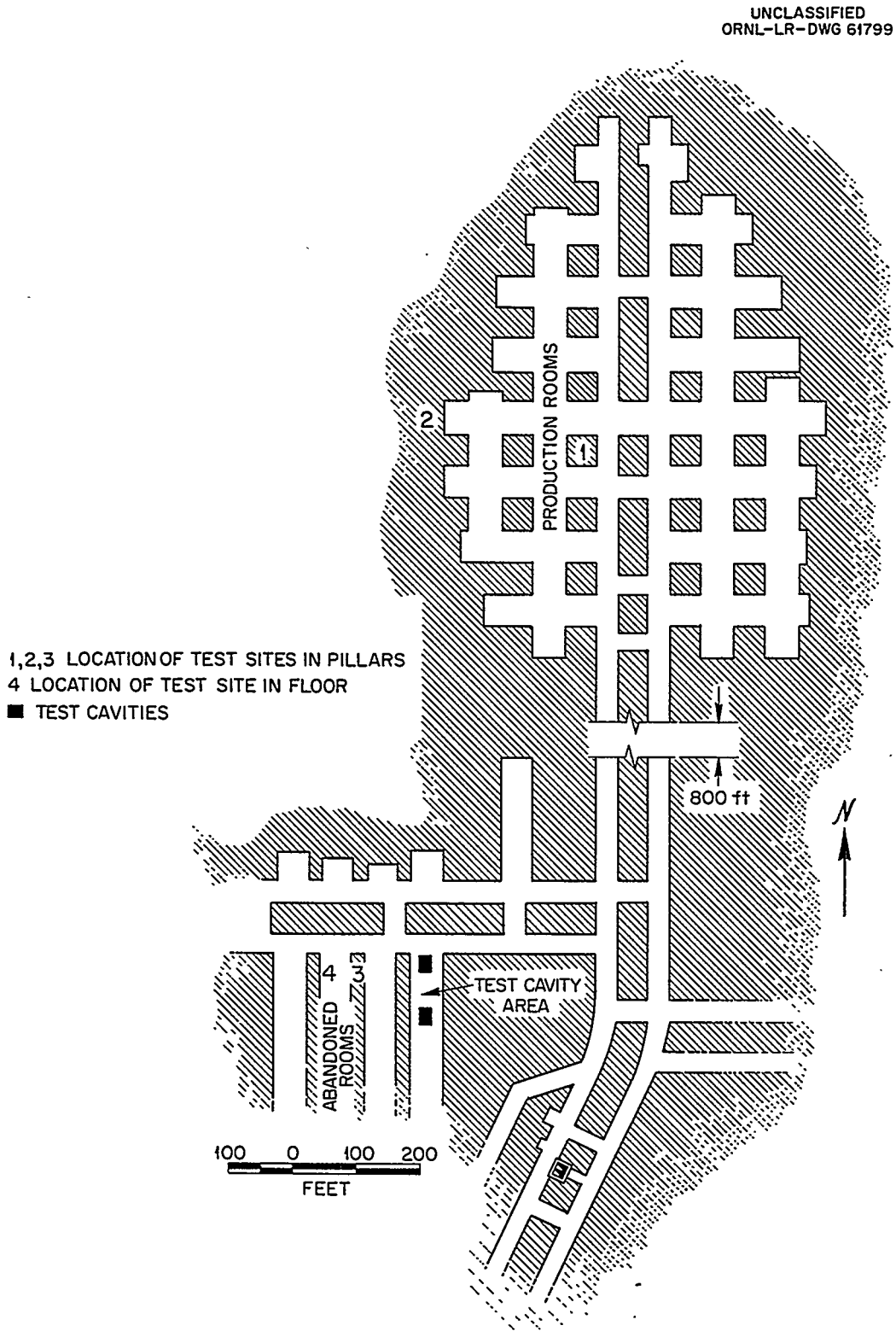

Fig. 6.4. Plan of Carey Salt Mine, Hutchinson, Kansas, Showing Location of Stress Measuring Stations.

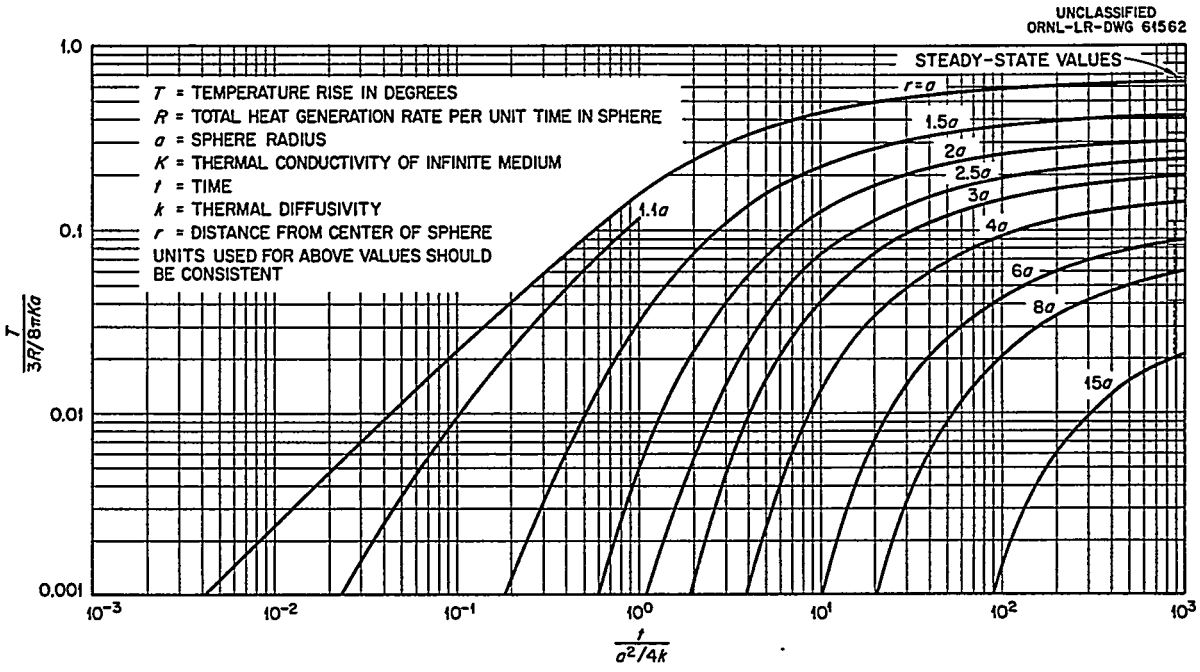

Fig. 6.5. Temperature Rise Around a Sphere with a Step Input of Heat Generation Rate.

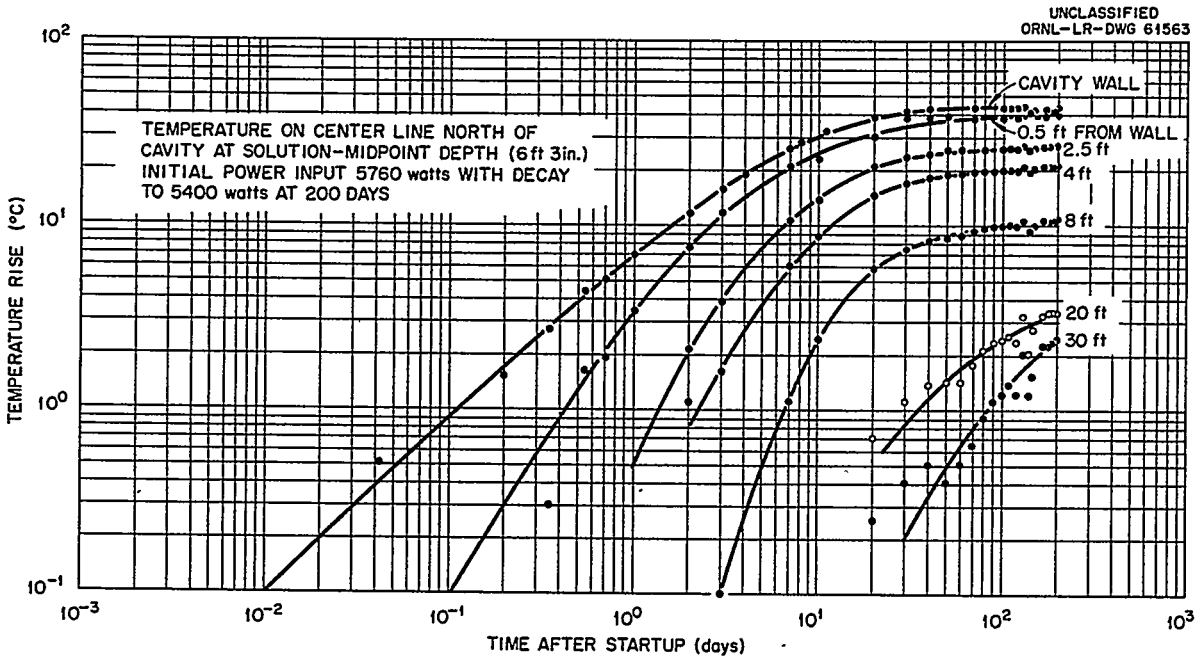

Fig. 6.6. Temperature Rise in 7.5-in. Cube of Waste.

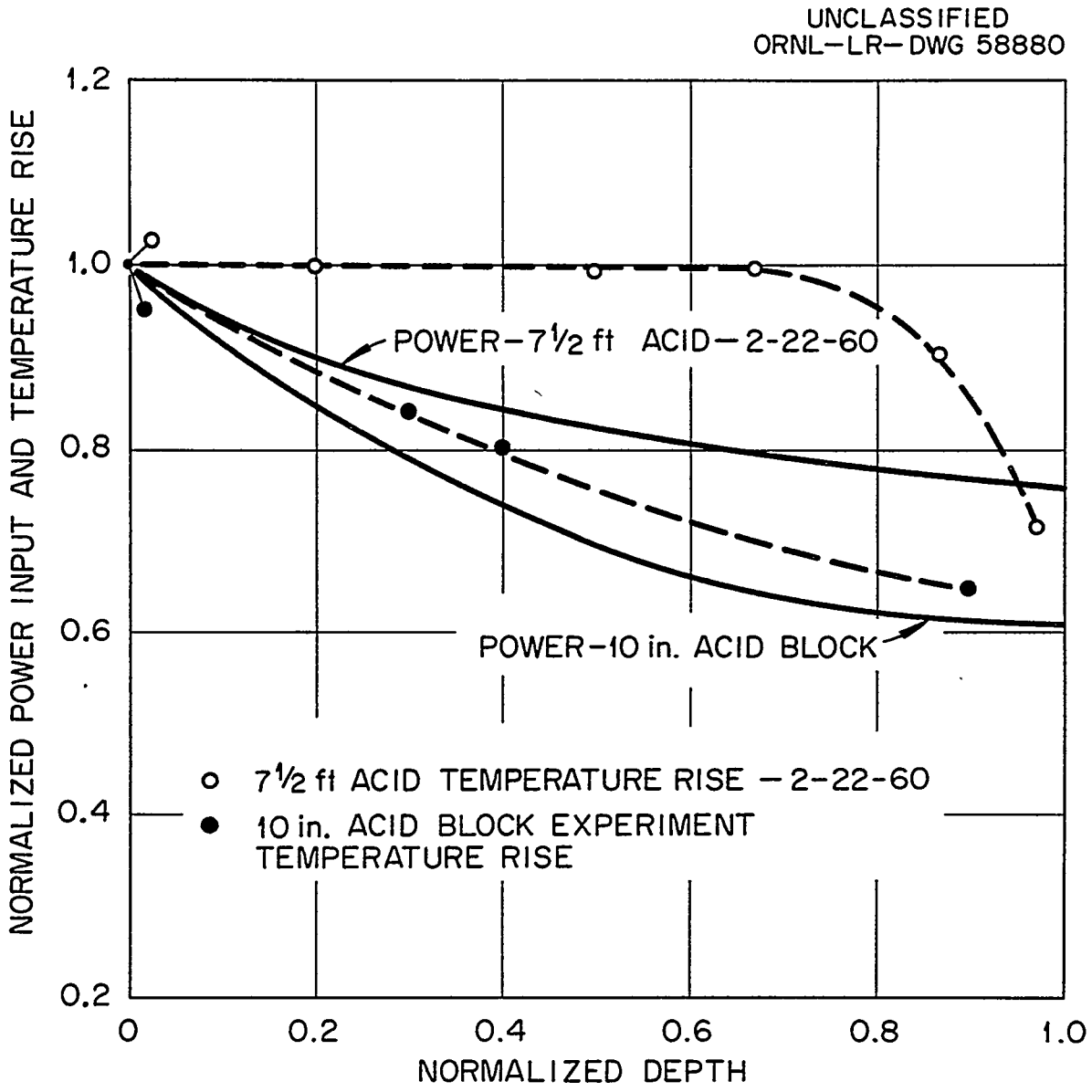

Fig. 6.7. Variation in Power Input and Temperature Rise with Depth.

In the neutralized waste there was a viscous precipitate, which settled to occupy approximately 30% of the solution volume. Heating was essentially confined to this region, since most of the fission products would be scavenged by the precipitate. There was little or no convection in the precipitate, and, consequently, temperatures as high as 120°C were recorded near the center; however, there was a steep gradient and temperatures at the cavity wall were approximately the same as in the supernatant region. There was free convection in the supernatant, and thereby, a uniform temperature distribution.

In September 1960 (approximately 8 months after the start of the test) five additional thermocouple holes were drilled to a depth of 30 ft on the north side of the neutralized waste cavity. The vertical temperature distribution in the cavity and out into the salt at the center of the north wall of the neutralized cavity is shown in Fig. 6.8. Temperature contours in the precipitate are based on data from five fixed-position thermocouples and vertical traverses made with two thermocouples and are therefore less accurate than the salt temperature contours. The contours in the salt were constructed from data obtained from 44 thermocouples. Insufficient thermocouples were installed to construct temperature contours around the acid cavity, but a comparison of existing thermocouples indicated that the temperature profile was approximately the same as for the neutralized cavity.

Slab Heat Sources. The new code designed for monitor runs on the IBM-7090 computer was checked, and results were obtained. The code is formulated so that the temperature rise is evaluated as a function of time for waste whose age at the time of burial varies. The temperature at any number of points in the heat-generating layer (waste mixed with salt) and in the infinite medium (salt) may be calculated. The vertical thickness of the heat-generating layer may also be varied. An assumption is made that equal amounts of heat flow upward and downward, so that the problem resolves itself to the semi-infinite region bounded by the plane $x = 0$, where x is the depth below the center of the waste layer. The general heat-conduction equations were thus set up with the following boundary conditions: (1) for $t < 0$, the temperature is zero throughout the region $0 \leq x < \infty$; (2) for $t > 0$, there is no flow of heat across the boundary at $x = 0$; (3) for $t > 0$ in the region $0 < x < a$ (where $2a$ = thickness of waste layer), heat is generated which is independent of position but dependent on time. The equations were solved by, first, dividing the total time in which the temperature structure is desired into finite intervals of length Δt. The rate of heat generation is assumed to be constant, and the differential equations are solved and the temperatures calculated at the end of each time interval. The temperatures due to heat impulses, starting at $t = n\Delta t$ and ending at $t = (n + t)\Delta t$, are then derived from the first result. The mean value of the heat input in each time interval, Δt, is calculated. By means of a finite approximation to a convolution intregral, the last two results are combined to yield the temperature rise due to the variable heat source.

In Fig. 6.9a are shown peak temperature rises at the center of the heat-generating layer ($x = 0$) as a function of decay time before storage, obtained with the slab code. The rate of heat generation decay used was that

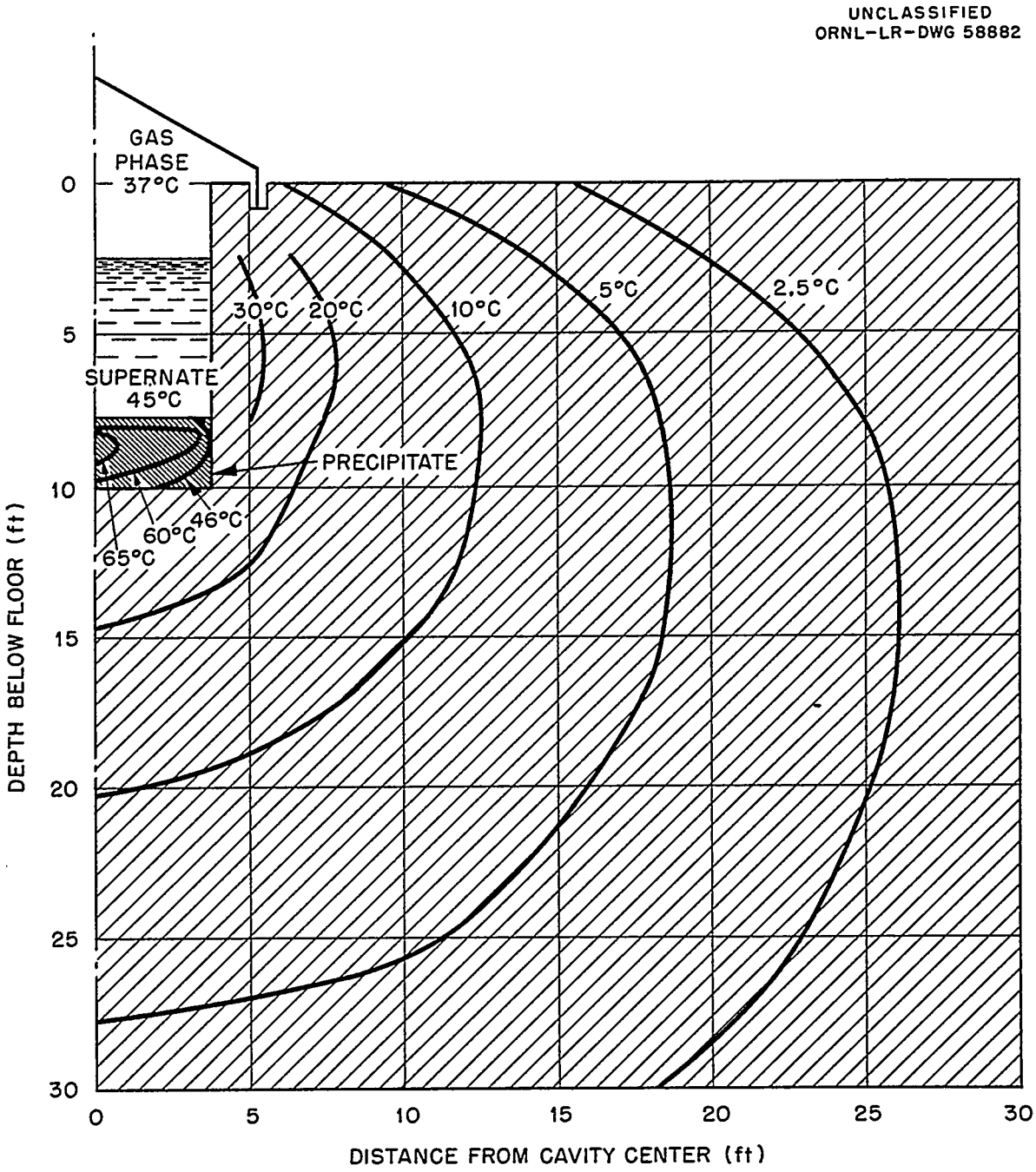

Fig. 6.8. Vertical Temperature-Rise Contours in 7.5-ft Cube of Neutralized Waste.

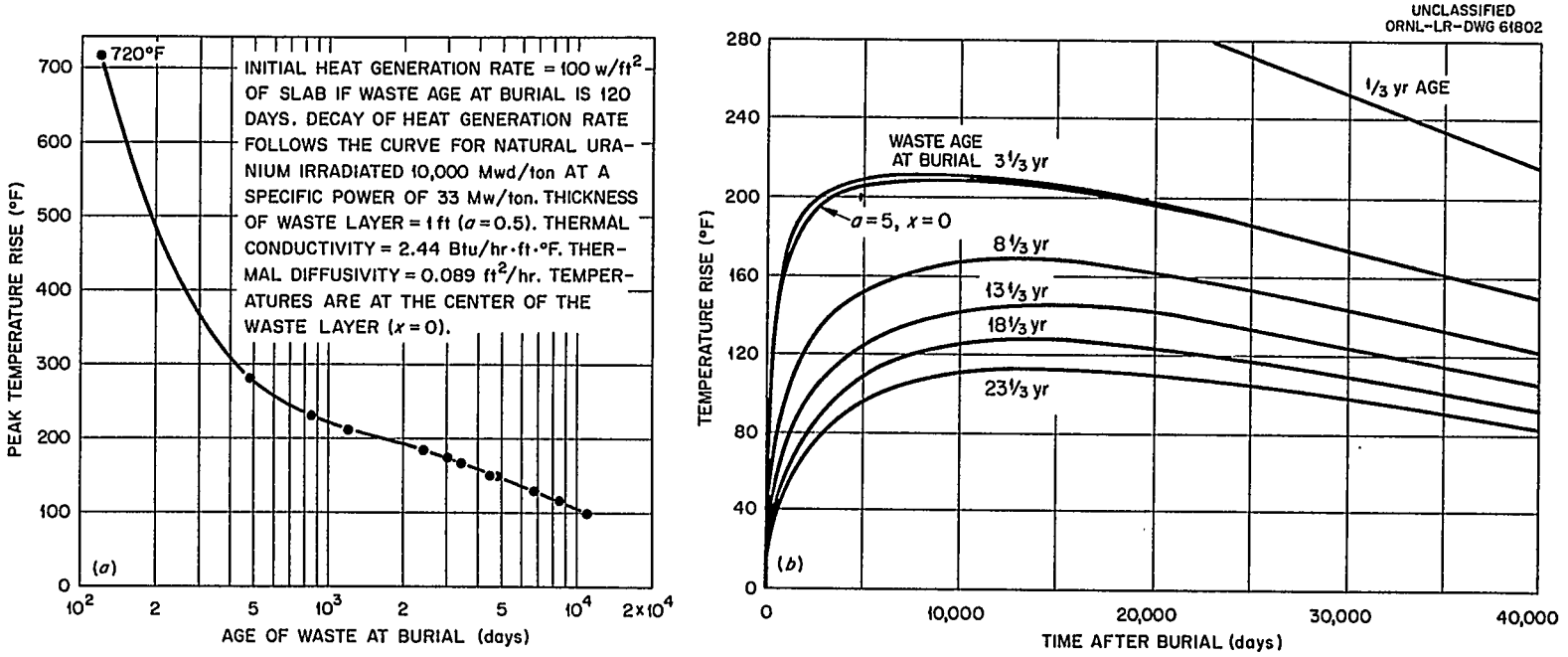

Fig. 6.9. (a) Peak Slab Temperature as a Function of Age of Waste at Burial. (b) Temperature Rise in Infinite Slab with Decaying Heat Source.

produced by natural or slightly enriched uranium fuel irradiated to 10,000 Mwd/ton at a specific power of 35 Mw/ton. The heat-generation rate in the slab was arbitrarily assumed to be 100 w/ft^2 for wastes of 120 days age at the time of burial, and the 100 w/ft^2 was assumed to be contained in a slab 1 ft thick (a = 0.5 ft). Thermal constants used were those for salt at a temperature of 100°C. Since the temperature rise is a linear function of the heat-generation rate per unit of slab area, so rises for wastes of different heat-generation rates per unit area may be obtained by multiplying by the appropriate factor. It is apparent from Fig. 6.9a that it would be wasteful of mine space to store wastes which have decayed less than 1 year.

In Fig. 6.9b are shown some temperature-rise versus time curves obtained for the same conditions as Fig. 6.9a with the exception that the second curve from the top applies for a layer of 10-instead of a 1-ft-thick layer. Comparison of the two top curves indicates that there is little thermal advantage to be gained from dispersing the waste in depth. The time to reach peak temperature in the slab varies from 175 days for 120-day-decayed wastes to 14,000 days for wastes aged 23 years before burial.

6.4 Salt Cavity Alterations (H. Kubota*)

Isothermal Erosion at 75°C. A salt block kept in a system where vapor, liquid, and solid phases were in thermal equilibrium at 75°C is shown in Fig. 6.10a. There is no erosion at the water line. The solid face that was in contact with the liquid has a cleaner surface and more uniform crystalline properties than the face that was in contact with the vapor phase. This is probably due to an exchange of salt between the solid and the solution, with the loss of the impurities present in the solid to the solution. The salt in contact with the vapor phase shows signs of partial dissolution, but the degree is much less than when the solution alone was heated.

Storage in Crushed Salt. Studies now under way indicate that radiolysis may be minimized by storing the waste solutions in the interstices of crushed salt The results of a study of this type of storage are shown in Fig. 6.10b. No changes in the wall of the block, in either the liquid or vapor phase, are apparent. The liquid level at the end of the test had dropped to about 80% of the original, the lost liquid being distributed throughout the salt layer above the liquid. One of the mechanisms of water movement evidently was vaporization followed by condensation on the cooler salt. There was considerable cohesion of the original loosely packed salt particles, which could have resulted from partial solution of salt followed by drying so that neighboring particles were fused together. Capillary forces also must have come into play, because the face of the block, as well as areas of the crushed salt, are mottled by the color of the synthetic waste solution up to the upper level of the crushed salt. The study indicates that very little cavity alteration would be expected from this type of storage.

6.5 Radiolytic Off-gas Studies (H. Kubota)

Radiolytic decomposition of synthetic Purex waste, partially neutralized to 1.2 M acid, and formaldehyde-denitrated Purex (0.5 M acid), to avoid the

---

*Analytical Chemistry Division, ORNL

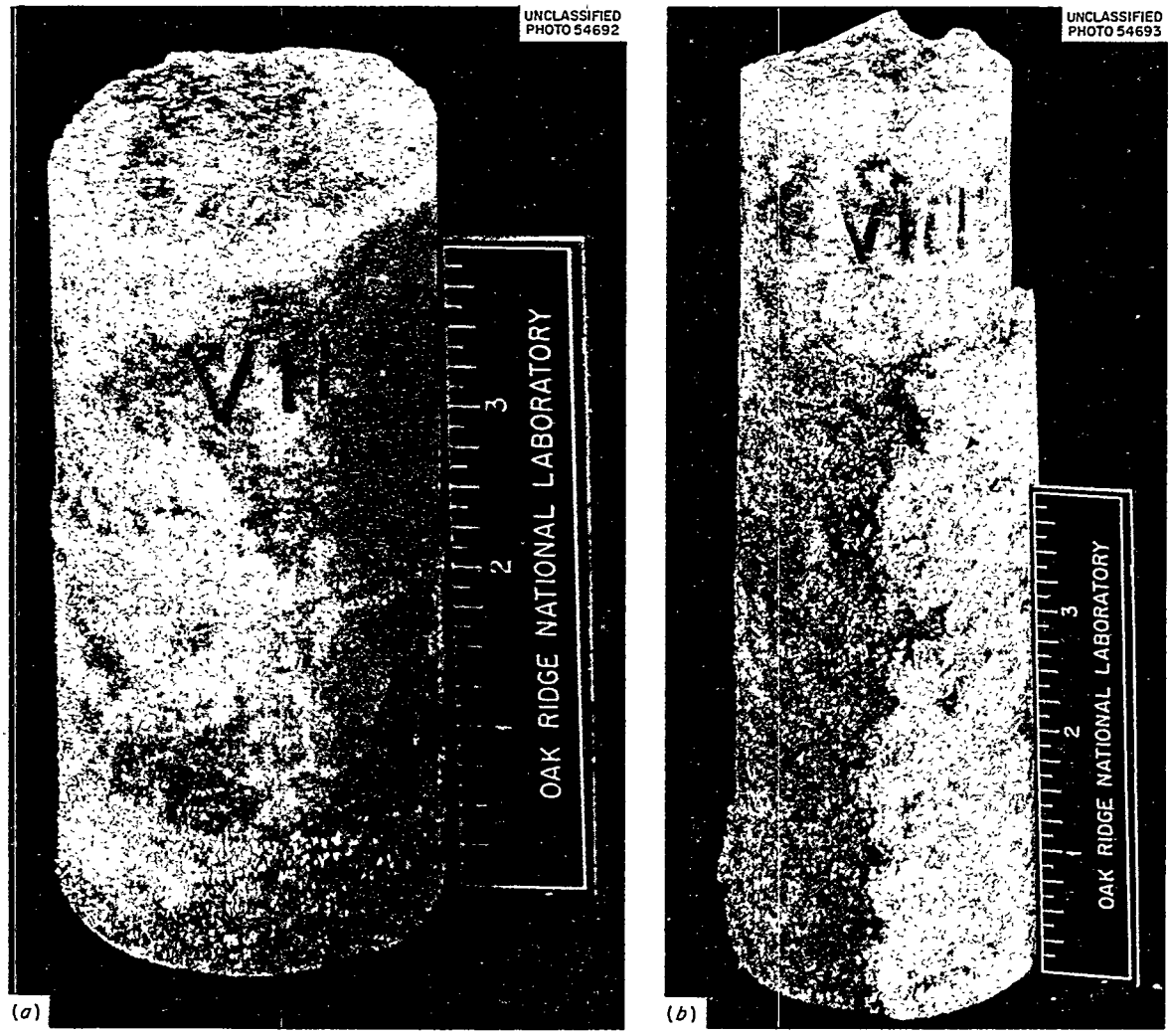

Fig. 6.10. (a) Salt Block Stored in System Where Vapor, Liquid, and Solid Phases Were in Thermal Equilibrium at 75°C; (b) Liquid Waste Stored in Interstices of Crushed Solid Salt.

possibility of chemical gas production, was studied. Waste solution in a confined system will approach steady state, where the recombination of product gases balances radiolytic dissociation, and will maintain this condition over a wide radiation dose range. This steady state is attained at pressures of 3-10 atms, depending on the composition of the waste solution.

It is probably impossible or impractical to maintain a pressure head of a few atmospheres in salt structures over long periods of time; therefore containment in a closed system with the expected pressure buildup is unlikely. A hydrogen atmosphere over the solution will decrease steady-state pressures to atmospheric levels. This, too, is considered impractical. Currently known recombination catalysts operate with increasing efficiency with increasing pressure. The minimum pressures at which favorable rates of recombination are realized are also too high for realistic application in salt structures. At present, therefore, the containment of liquid wastes in salt cavities can be expected to result in the production of radiolytic gases, principally hydrogen and oxygen.

In a different approach to the study of salt cavity storage of liquid wastes, minimizing radiolysis as well, the possibility of suspending the waste solution as surface films on crushed salt was considered. Waste solution was poured over crushed salt at a ratio of 1 ml/5 g of salt. The salt and solution were contained in an irradiation tube of the type shown in Fig. 6.11. Upon exposure to Co-60 radiation no pressure was built up as long as the liquid remained suspended in the solid phase. As the dose approached 10^9 rads, a liquid phase formed over the solid salt layer in most of the tubes. This phase separation was accompanied by a buildup in pressure. In order to minimize possible wall effects, the same irradiation was repeated in larger tubes containing five times more salt. The behavior was the same, which strengthens the thought that phase separation is more closely associated with radiation effects than container wall effects. Varying the particle size caused no change in the radiolytic process. When coarse salt particles (1/2 in.mesh) were used, there were relatively large volumes of free solution in the void spaces. Despite the existence of such locales of free solution, no radiolytic pressure built up as long as the free liquid was overlaid by a layer of salt.

When waste solution was sorbed on vermiculite and attapulgite, the radiolytic behavior was similar. The maximum pressure buildup was 20 mm Hg at 10^9 rads.

7.0 CLINCH RIVER STUDY

7.1 Water Sampling and Analyses (P. H. Carrigan*)

At the Clinch River Study Steering Committee Meeting, May 4, 1961, members of the Subcommittee on Water Sampling and Analysis suggested the installation of a continuous proportional sampler on the Clinch River at

*On loan from Tennessee District, Surface Water Branch, Water Resources Division, U. S. Geological Survey.

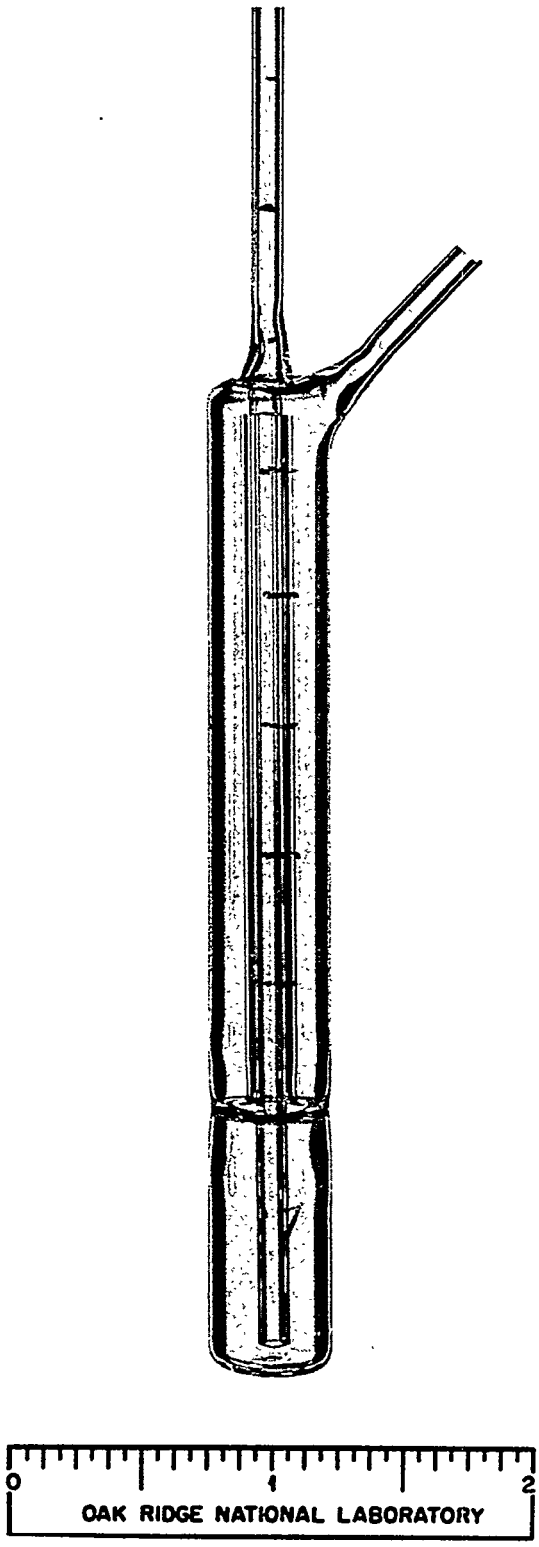

Fig. 6.11. Irradiation Cell, 5 ml Capacity.

Centers Ferry (CRM 5.5). An alternative sampling system, designed by engineers of the ORNL Instrumentation and Controls Division, was installed. It consists of a U.S. Geological Survey electromagnetic velocity meter, null-balancing potentiometer, a Variac speed controller in the armature circuit of a d-c shunt motor, and a finger pump. The flow rate through the pump is proportional to the velocity of flow in the river. At Centers Ferry, where the flow is stratified, the warm, upper stratum may be still-water at times during the summer. The colder stratum (water discharged at Norris Dam), flowing near the bottom of the channel, will be sampled, and the sensing probe of the velocity meter and the intake to the pump were placed 200 ft from the right bank, 40 ft below the surface, in the deepest part of the cross-section. The measured velocity and analyses of water samples will be compared to the average velocity and average water quality distribution at the cross-section as determined by current-meter discharge measurements made at frequent intervals to determine whether the continuous point sample is representative of average conditions.

Each water sample is filtered through a 0.5 μ pore membrane filter, and the filter residue and filtrate are analyzed separately. The results of a series of tests to determine the extent of radioisotope sorption on the filter indicated that less than 0.5% of the strontium, cobalt, or ruthenium and only 4% of the cesium present in water samples are sorbed. The Cs-137, Co-60 and Sr-85 solutions added to the samples were obtained from the ORNL Isotopes Division. The ruthenium solution was obtained from the seepage streams of the ORNL waste pits, as it was felt that environment effects on the chemical state of ruthenium should be included in the tests. The concentration of each radionuclide in 1 liter of uncontaminated, filtered river water was adjusted to approximate levels of activity found in Clinch River water, and the solution was passed through the filter and discarded. The filter was washed with a small known volume of concentrated hydrochloric acid, and the activity in the acid wash determined.

7.2 Bottom Sediments (P. H. Carrigan, W. E. Parker, J. A. Payne)

The Clinch River Study Subcommittee on Bottom Sediments recommended that (a) the distribution of bottom sediment volume and radioactivity in bends of the Clinch River be studied, (b) an evaluation of bottom sediment core samplers be undertaken, (c) core samples at five well-spaced sections be obtained for physicochemical analyses, and (d) methods for determining total sediment volume be verified.

a. Initial field work on distribution of bottom sediment volume and of radioactivity of these sediments was done at one of the sharpest bends in the Clinch River, between CRM 5.4 and 6.3, at these and four intermediate sections.

b. Ten types of core samplers were compared and evaluated for compaction and retention of sediment samples. The most effective sampler was found to be a 3.5-in.-dia split-tube sampler with basket shoe. Each of the 10 types was selected on the basis of method by which the sampler is drilled into the sediment or the method by which the core is retained as the sampler is withdrawn from the sediment. Several diameters of the sampler tubes were selected to determine the effect of tube diameter on compaction of the core.

c. Previous work has shown that the concentration of radioactivity in Clinch River bottom sediments decreases rapidly within the first mile of river downstream from the mouth of White Oak Creek (17,18). The concentration then increases to a secondary maximum about 10 miles downstream. Downstream from the secondary maximum the concentration decreases almost linearly with distance. This variation in concentration is unexplained.

Core samples of the bottom sediments were obtained from five, well-spaced sections for the purpose of determining physicochemical factors that might influence these variations in concentration. At each section a composite of 10 cores were prepared for analyses. The analyses will include particle-size distribution, exchange capacity, sorption capacity, and mineralogy. Sorption capacity determinations will be done at ORNL; and the other analyses at laboratories of the U.S. Geological Survey.

d. At five-year intervals TVA makes a survey of sediment volume in the Clinch River by means of sediment area and water area measurements at five carefully selected cross-sections in the river. At the request of the Subcommittee on Bottom Sediments, four intermediate sections were included in the 1961 survey. Results of this survey show that there is no significant change in water volume, and hence in silt volume, even if the four intermediate sections are included in the computations.

7.3 Distribution Coefficient Determinations (T. Tamura)

The sorption of cesium and strontium from tap water by several clay minerals was measured (Table 7.1). Vermiculite and illite showed very high affinities for cesium; the reasons for this have been documented earlier (19). The high removals by vermiculite (actually a hydrobiotite, with 50% biotite and 50% vermiculite interstratified) show that the sorptive capabilities of this mineral were previously underestimated (18). The increase noted here is undoubtedly caused by the smaller particles (less than 50 μ dia) used in these tests compared to the particles of approximately 300 μ dia used earlier. None of the ion exchange sites of kaolinite and montmorillonite have steric properties for the exclusion of the gross ionic constituents of tap water. Thus, the partial cesium capacities of these minerals are more sensitive to the ion impurities of the tap water than either illite or vermiculite, which do have highly selective edge features.

Strontium sorption was greatly influenced by the calcium and magnesium in tap water since the reaction is largely controlled by the single mass action relation. Kaolinite, which, despite its low ion exchange capacity, sorbed a relatively high amount of strontium from demineralized water, is thought to have a high selectivity for strontium because of its higher hydroxyl content. However, the number of hydroxyls that may be involved in the reaction is too small to accommodate all the calcium and magnesium ions present in tap water. This response of kaolinite for strontium resembles the response of illite for cesium; in both cases the reactions appear to involve elements at edge or near-edge sites. Kaolinite-strontium selectivity is different in that the reaction is reversible and highly sensitive to changes in pH.

Table 7.1 Removal of Cesium and Strontium by Several Clay Minerals from Demineralized Water and Tap Water

Test condition: 0.1 g of mineral per 200 ml of solution

Material	Contact Time, hr	Cesium				Strontium			
		Activity Sorbed (%)		Distribution Coefficient, K_d*		Activity Sorbed (%)		Distribution Coefficient, K_d*	
		Demineralized Water	Tap Water	Demineralized Water	Tap Water	Demineralized Water	Tap Water	Demineralized Water	Tap Water
Vermiculite	1	98.6	97.6	140,000	82,500	34.8	15.5	1,100	370
	4	97.2	98.0	68,600	98,100	44.2	17.8	1,600	430
	24	98.8	98.5	165,000	134,000	47.8	19.4	1,800	480
	168	98.8	98.6	169,000	146,000	46.5	19.4	1,700	480
	432	99.4	98.9	352,000	181,000	53.4	20.2	2,300	510
Illite	1	81.2	85.5	8,700	11,800	84.3	14.1	10,700	330
	4	88.0	83.2	14,700	9,900	85.7	15.1	12,000	350
	24	93.3	88.7	27,800	15,700	83.0	14.8	9,700	350
	168	97.3	93.6	72,100	29,100	73.4	16.7	5,500	400
	432	97.6	96.1	79,800	48,800	74.1	17.7	5,700	430
Kaolinite	1	63.1	23.4	3,400	610	17.4	4.34	420	90
	4	58.3	20.0	2,800	501	23.2	4.15	600	90
	24	58.0	21.2	2,800	540	24.0	5.89	630	125
	168	55.7	23.7	2,500	620	22.3	5.72	570	120
	432	53.8	20.9	2,300	530	18.9	5.52	470	115
Montmorillonite	1	44.4	23.0	1,600	600	59.3	2.42	2,900	50
	4	34.8	16.4	1,100	390	61.4	3.56	3,200	75
	24	33.8	21.0	1,000	530	58.5	2.01	2,800	40
	168	36.2	22.1	1,100	570	51.8	1.58	2,200	30
	432	46.3	20.0	1,700	500	50.8	2.66	2,100	55

*K_d = $\frac{\text{fraction sorbed per g of material}}{\text{fraction remaining per ml of solution}}$

Considering the amount of strontium in the tagged solution, it is estimated that the calcium concentration in tap water represents 10,000 strontium ions. The amount of potassium in the tap water is equivalent to 20,000 cesium ions. Thus, though more cesium equivalent is represented by the potassium ion concentration in tap water, its influence on cesium uptake is much less than the influence of calcium on strontium uptake.

Clinch River sediments are principally illitic, with smaller amounts of kaolinite and vermiculite; any K_d determination will give values of about 100-150 depending on the relative amounts of kaolinite and vermiculite. Based on a K_d for strontium of 150, it is estimated that the suspended sediment load necessary to sorb 5% of the strontium in the river would be of the order of 350 ppm.

For these tests tap water was used instead of Clinch River water since they are quite similar in chemical composition:

Water	Ion, ppm					
	Ca^{++}	Mg^{++}	Na^{+}	K^{+}	HCO_3^{-}	$SO_4^{=}$
Clinch	22.4	6.8	2.6	1.4	110	11.1
Tap	26.0	5.5	6.1	1.1	97	---

The pH of the simulated river water was adjusted to 7; upon contact with the mineral the pH in almost every case rose and remained between pH 7.5 and 8.0. Samples were taken at 1 hr, 4 hr, 24 hr, 7 days and 18 days after contact. Distribution coefficients (K_d) were calculated and compared with those obtained in demineralized water.

8.0 FUNDAMENTAL STUDIES OF MINERALS

8.1 Sodium-treated Vermiculite (T. Tamura)

The results of experiments in the pH range 2 to 11 showed that pH has a strong influence on the sorption of strontium by Na-vermiculite (Fig. 8.1). The Na-vermiculite was prepared by leaching twice with NaCl solution followed by two treatments with NaCl-NaOH solution. The sorption curve shows three distinct responses: a sharp rise between pH 2 and 4.5, very little change between pH 4.5 and 9, and another increase at pH 11.

Between pH 2 and 4.5 the effect of contact time was significant. Above pH 4.5 sorption was increased by increasing the contact time from 24 to 96 hr; below pH 4.5 the effect was reversed. At pH 4 sorption was maximum (62%) after 48 hr; hence, it is expected that longer contact time will continue to decrease the sorption of strontium. The cause of this reduction in sorption is the instability of clay minerals below pH 4.

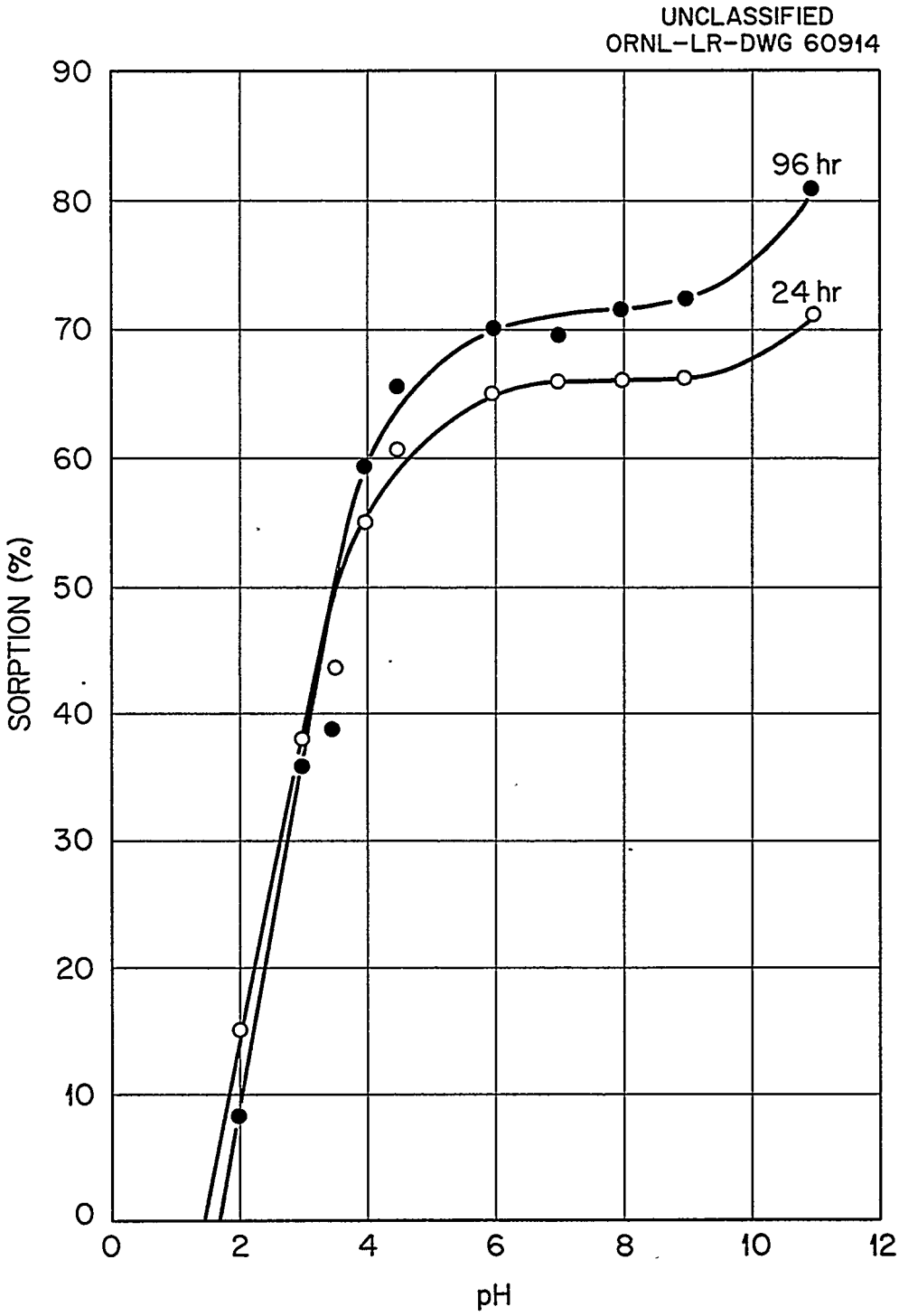

Fig. 8.1. Removal of Strontium by Na-Vermiculite as a Function of pH. Simulated Waste: 0.1 N $NaNO_3$ containing 1 mg of Sr^{2+} per liter; 100 ml of solution per gram of vermiculite.

Between pH 4.5 and 9 there was very little difference in sorption, which suggests that the attractive force for the strontium ion is the negative charge resulting from the isomorphous substitution of aluminum for silicon. Earlier tests with vermiculite treated with NaCl showed differences only between pH 7 and 9, probably because of the incomplete removal of exchangeable magnesium and calcium ions.

The rise at pH 11 is difficult to explain. In tests on simple pH effect, at pH 11 about 3% of the strontium was removed by centrifugation of the waste solution. The removal at pH 11 was dependent on the previous history of the vermiculite; e.g., on the number of NaCl treatments and the concentrations of the NaCl solution (Table 8.1). With eight increments (7500 meq of Na ions per 50 g of vermiculite), the response at pH 11 was the same as with the sample treated twice with NaCl and twice with NaCl-NaOH solution. This suggests that exchange capacity is not the primary cause for the increase. More work is necessary to establish the factor(s) responsible.

Table 8.1 Effect of Pretreatment on Strontium Removal by Vermiculite

Test conditions as shown in Fig. 8.1; pH = 11; vermiculite initially sodium saturated with NaCl

No. of Increments*	Sr Removal (%)				Exchange Capacity (meq/100g)
	1 hr	4 hr	24 hr	71 hr	
NaCl					
0	26.0	40.3	59.9	65.5	69.5
2	26.6	43.4	65.5	68.2	66.5
4	26.2	44.6	69.1	72.4	65.3
8	28.6	47.8	74.7	79.4	64.5
13	29.0	46.2	72.9	78.9	66.0
NaCl-NaOH					
2	26.4	45.2	72.1	79.1	71.5

*An increment is equal to 750 meq of Na as NaCl and 350 meq of Na as NaCl-NaOH per 50 g of material.

8.2 Removal Efficiency Comparisons (T. Tamura)

The removal efficiencies of natural alumino-silicates were compared with synthetic organic resins. Of the materials tested (Table 8.2), only vermiculite was treated prior to use (NaCl and NaCl-NaOH treatments). At low pH vermiculite decomposed and was ineffective as a strontium sorber. The other alumino-silicate, clinoptilolite, showed a slight decrease at pH 2, while the organic

resins performed effectively in the entire pH range investigated. There was a noteworthy difference between materials of high exchange capacity such as Dowex 50 (500 meq/100 g) and vermiculite (70 meq/100 g). The exchange capacity of Dowex 50 and Duolite C-3 results from the ionization of functional groups making up the resins; with clinoptilolite and vermiculite the exchange arises from isomorphous substitution of aluminum ions for silicon.

Table 8.2 Strontium Removal from Sodium Nitrate Solution

50 ml of 0.1 N $NaNO_3$ solution containing 0.05 mg of Sr;0.5 g of sorbent.

pH	Contact Time (hr)	Sr Removal (%)			
		Clinoptilolite	Duolite C-3	Dowex 50W X12	Na-Vermiculite
11.0	24	83.7	84.9	96.6	69.0
	71	93.8	95.0	96.8	81.6
9.0	70	89.6	90.2	97.4	71.2
	94	91.2	90.9	97.4	74.1
4.0	24	77.4	84.9	94.3	50.6
	71	90.5	90.5	97.7	60.3
2.0	24	65.1	85.3	96.6	13.3
	96	84.5	90.6	97.6	7.84

8.3 Soil Columns (D. G. Jacobs)

Cesium breakthrough curves obtained from vermiculite-filled columns* are complicated by a particle-diffusion rate-controlling process. This is shown by the prolonged time required for the concentration of the effluent to reach zero gradient after the inflection of the breakthrough curve and results in increased loading of cesium on the column with increased time of operation.

Glueckauf (20) has given a mathematical treatment for the effect of particle diffusion on the effluent concentration history from columns filled with spherical resin beads of uniform particle size. However, the vermiculite particles are not spherical but are flaky like mica (isinglass). The exchanging cesium must find its way to basal exchange sites by migrating from the edge of the vermiculite flakes; migration through the faces of the platelets is prevented by the crystal structure of the vermiculite. The commercially available grades of vermiculite are not of a single uniform particle size but have a normal distribution of particle sizes. Thus, the mathematical model presented by Glueckauf was extended to take these two factors into consideration.

*Hydrobiotite obtained from the Zonolite Company, Traveler's Rest, South Carolina.

Particle diffusion coefficients were estimated (Table 8.3) by comparing the concentration histories of experimental columns with theoretical curves. Slopes at various points along the breakthrough curve were compared and the particle diffusion coefficient was estimated from effluent data. The experimental data do not show a constant value for the particle diffusion coefficient, D. Some possible factors accounting for this may be: (a) This is a natural exchanger material having more than one type of exchange site; thus the kinetics observed for the system are the net result of those of several separate processes. (b) In the collapsed layer lattice minerals, it is not uncommon for the periphery of the particle to have a somewhat greater basal spacing than the core of the particle, due to a gradually increasing degree of hydration toward the outside of the particle (21); this would mean less steric impedance to the diffusing ion near the periphery of the particle and D would decrease as the diffusing species moved toward the interior of the particle with time. (c) Initially, the major saturating cations of the vermiculite are magnesium and potassium; as column operation proceeds, these cations are gradually replaced by sodium, the major cationic constituent of the influent solution. Thus, the ion population in the zone of restricted cesium movement is continuously being altered and affecting the diffusion of cesium because the ion population of exchange sites measurably affects the interlayer spacing.

All these factors could be operative, and the net effect would be an increase in the apparent surface K_d and a decrease in the apparent diffusion coefficient with increased time of column operation.

It has already been noted that particle diffusion affects the concentration history of the effluent from an ion exchange column; that is, at high percentage breakthrough the concentration gradient dimminishes but approaches zero gradient rather slowly. This is of little consequence in the loading of an ion exchange column where the concern is only for very low breakthrough percentages. A second effect, increased loading of the column with increased operating time, would be of concern. The time required to attain equilibrium between the interstitial solution and the interior of the particle is a function of the particle size; so the choice of vermiculite grade (grading is based on the particle size distribution) would be somewhat dependent on the predicted operating time of the column.

Another interesting point is that particle diffusion will result in "recovery" of a column. When the loading operation is temporarily halted, a portion of the surface cesium migrates to the interior exchange sites and results in cesium deficiency at the particle surface. Replenishment of the surface cesium, when operations are resumed, results in a decrease in the effluent activity from what it had been immediately before the operation had been stopped. This behavior will continue until the interior of the particle approaches equilibrium with the surface. Flow rate also has a pronounced affect on the effluent quality because it affects the time allowed for diffusion of the cesium to the interior exchange sites of the vermiculite.

Table 8.3 Estimation of Particle Diffusion Coefficients From Experimental Concentration Histories

Column No.	Wt (g)	Ht (cm)	Flow Rate (ml/min)	θ* (hr)	N**	HETP (cm)	Surface K_d (ml/g)	D x 10^{11} (cm^2/sec)
2	94.7	18.9	3.8	64	68	0.28	163	2.7
3	99.0	19.3	7.6	26	97	0.20	120	8.1
4	98.4	21.7	16.7	8.9	50	0.44	103	11.5
5	97.6	20	57.7	2.0	39	0.52	76	86.6
6	48.1	11.8	5.2	20	54	0.22	140	12.9
7	54.2	11.5	4.8	25	44	0.26	137	10.0
8	190.5	45.8	5.1	102.	192	0.24	207	4.0
9	291.6	70.9	5.2	234	406	0.17	229	2.7

*θ is the time required to reach the inflection point of the breakthrough curve.

**N is the number of theoretical plates or transfer units in the exchange column.

9.0 WHITE OAK CREEK BASIN STUDY

9.1 Sources of Contamination in White Oak Creek (T. F. Lomenick)

White Oak Lake formerly served as a final settling basin for low-level radioactive wastes discharged from ORNL. White Oak Dam, a highway fill located 0.6 mile upstream from the confluence of White Oak Creek and the Clinch River, was closed in October 1943. The lake extended about 1 mile upstream and covered an area of about 44 acres. The temporary holdup afforded some dilution and time for the decay of short-lived radionuclides before release to the Clinch River; it also allowed the deposition and accumulation of contaminated sediments. By draining the lake in 1955 and allowing the gate at the dam to remain open, the creek now flows unimpeded into the river. At present, there is a 100,000-ft^3 impoundment behind the dam. Seepage from the waste pits flows onto the lake bed, and radionuclides from the lake bed enter the creek.

To determine the nature and extent of fission product accumulation and transport in the lake bed, geologic and hydrologic investigations are needed, as well as information on the quantity and distribution of radionuclides already in the bed.

The lake bed is underlain by 6 to 12 ft of alluvial material and the Conasauga shale formation of Cambrian age. The alluvial material consists mostly of silts and clays; however, some sands and gravels are present. Core samples, taken to a depth of 6 ft along transects at the upper, middle, and lower parts of the bed, and auger samples, taken at depths below 6 ft, are being mechanically analyzed to determine the particle size distribution.

To define the configuration of the water table, 31 shallow observation wells have been completed in the lake bed. These wells, which vary from 5 to 6 ft in depth, consist of a perforated casing surrounded by gravel. The direction and rate of ground-water movement within the area will be assessed by mapping the water table and by laboratory and field tests of soil permeability.

A sampling program has been initiated to determine the vertical and lateral distribution of radionuclides in the lake bed. For the first phase of this program, fifteen 6-ft-deep core samples were taken along three monumented silt ranges: one at the upper end, one in the middle, and one at the lower end of the lake. The samples were recovered with a 2-in.-dia thin-wall tube that was manually pressed into the soil. The cores were segmented into various increments for radionuclide analyses. In general, in the first 6 in. of soil, 1-in. increments were analyzed separately. At greater depths larger increments were used. A summary of the gross gamma activity in these cores, taken along the upper and lower ranges, is shown in Table 9.1. In general, more gamma activity per gram of soil was detected at the upper transect than at the lower one, most of the gamma activity was contained in the first 12 in. of soil, and activity in the upper few inches of each core was rather unifformly distributed. A more complete understanding of the distribution of radionuclides will be obtained by analyzing these cores for specific radionuclides.

Table 9.1 Distribution of Gross Gamma Activity in White Oak Lake Bed

Depth (in.)	Activity (c min^{-1} g^{-1} wet wt)									
	Upper Transect (White Oak Creek Mile 1.3)					Lower Transect (White Oak Creek Mile 0.9)				
	50 ft[a]	80 ft[a]	140 ft[a]	190 ft[a]	240 ft[a]	90 ft[a]	190 ft[a]	250 ft[a]	340 ft[a]	410 ft[a]
0 - 1	21,300	36,500	16,700	32,500	18,500	3,000		15,700	8,000	8,700
1 - 2	19,800	30,600	29,400	28,000	13,700	6,000	14,000[b]	14,400	9,600	13,400
2 - 3	19,600	20,500	29,200	27,000	21,400	2,100		13,400	18,100	13,700
3 - 4	190	18,400	31,700	28,000	21,000	450	13,800[c]	18,700	24,500	14,400
4 - 5	110	23,800	27,800	25,000	20,500	15			26,100	16,500
5 - 6	10	63,000	21,400	43,100	11,000	15	17,300[d]	1,300[d]	24,400	13,000
6 - 9	10	57,900	23,500	21,000	4,900	230	2,100	65	3,300	2,900
9 - 12	6	8,700	28,600	5,500	3,200	5	450	10	100	700
12 - 18	35	1,400	6,800	2,000	1,500	15	300	---	80	95
18 - 24	30	800	1,800	500	1,400	5	7	450	7	30
24 - 36	2	600	300	400	1,400	5	100	6	10	5
36 - 48	2	180	100	270	750	5	3	10	7	5
48 - 60	750	50	75	170	630	2	3	2	8	6
60 - 72	90	25	85	200	700	3	5	3	3	15

[a] Distance from left bank

[b] 0 - 2 in. depth

[c] 2 - 4 in. depth

[d] 4 - 6 in. depth

REFERENCES

1. "Chemical Technology Division Annual Progress Report for Aug. 31, 1960," pp. 93-95, ORNL-2993.

2. R. E. Blanco and E. G. Struxness, "Waste Treatment and Disposal Progress Report for April and May 1961," ORNL-CF-61-7-3.

3. Unit Operations Monthly Report, November 1960, CF-60-11-38.

4. Unit Operations Monthly Report, March 1960, CF-60-2-56.

5. Unit Operations Monthly Report, June 1961, CF-61-6-70.

6. Unit Operations Monthly Report, May 1961, CF-61-5-95.

7. J. R. Van Wazer, "Phosphorus and its Compounds," Vol. 1, Interscience, New York, 1958, p. 380.

8. A. D. Mitchell, J. Chem. Soc., 125: 1013 (1924).

9. B. Blaser, Z. physik, Chem. A166: 64 (1933).

10. Chemical Technology Section B, Monthly Report for March 1961, ORNL-CF-60-4-108.

11. "Chemical Technology Division Annual Progress Report for Aug. 31, 1961," ORNL-3153.

12. J. T. Roberts and R. R. Holcomb, "A Phenolic Resin Ion-exchange Process for Decontaminating Low-radioactivity-level Process Water Wastes," presented at Am. Chem. Soc. Meeting, New York, Sept. 11-16, 1960, ORNL-CF-60-8-103); (b) ORNL-3036 (May 22, 1961) gives more details.

13. R. R. Holcomb and J. T. Roberts, "Low-level Waste Treatment by Ion Exchange. II. Use of a Weak Acid, Carboxylic-Phenolic Ion Exchange Resin," ORNL-CF-61-3-114 (in preparation).

14. J. J. Perona, R. L. Bradshaw, J. T. Roberts, and J. O. Blomeke, "Evaluation of Ultimate Disposal Methods for Liquid and Solid Radioactive Wastes. Part II. Conversion to Solid by Pot Calcination," ORNL-3192 (in press).

15. H. S. Carslaw and J. C. Jaeger, "Conduction of Heat in Solids," 2nd ed., Oxford Press, London, 1959, p. 378.

16. F. Birch and H. Clark, "Thermal Conductivity of Rocks and its Dependence upon Temperature and Composition," Am. J. Sci. 238: 529-558, 613-635 (1940).

17. W. D. Cottrell, "Radioactivity in Silt of the Clinch and Tennessee Rivers," ORNL-2847 (Nov. 18, 1959).

18. R. J. Morton (ed.), "Status Report No. 1 on Clinch River Study," ORNL-3119 (July 27, 1961).

19. T. Tamura and D. G. Jacobs, "Structural Implications in Cesium Sorption," Health Physics 2: 391-398 (1960).

20. E. Glueckauf, "Theory of Chromatography, Part 10: Formulae for Diffusion into Spheres and Their Application to Chromatography," Trans. Faraday Soc. 51: 1540 (1955).

21. D. M. C. MacEwan, "Some Notes on the Recording and Interpretation of X-ray Diagrams of Soil Clays," J. Soil Sci., 1: 90-103 (1949).

DISTRIBUTION

1-2. R. E. Blanco
3. J. O. Blomeke
4. W. J. Boegly, Jr.
5. R. L. Bradshaw
6. J. C. Bresee
7. F. N. Browder
8. K. B. Brown
9. P. H. Carrigan
10. W. E. Clark
11. K. E. Cowser
12. F. L. Culler
13. W. de Laguna
14. F. M. Empson
15. D. E. Ferguson
16. H. W. Godbee
17. H. E. Goeller
18. J. M. Googin
19. C. W. Hancher
20. R. F. Hibbs
21. R. R. Holcomb
22. J. M. Holmes
23. D. G. Jacobs
24. W. H. Jordan
25. H. Kubota
26. T. F. Lomenick
27. K. Z. Morgan
28. R. J. Morton
29. E. L. Nicholson
30. F. L. Parker
31. J. J. Perona
32. R. M. Richardson
33. J. T. Roberts
34-35. E. G. Struxness
36. J. C. Suddath
37. J. A. Swartout
38. T. Tamura
39. J. W. Ullmann
40. M. E. Whatley

EXTERNAL

41. E. L. Anderson, AEC, Wash.
42. W. G. Belter, AEC, Wash.
43. J. A. Buckham, ICPP
44. H. J. Carey, Jr. (Carey Salt Co.,Hutchinson,Kansas)
45. C. W. Christianson, LASL
46. V. R. Cooper, AEC, Wash.
47. E. F. Gloyna (U. of Texas, Austin)
48. L. P. Hatch, Brookhaven
49. W. B. Heroy,Sr.(Geotechnical Corp.,Dallas,Texas)
50. H. H. Hess, (Chm. Earth Science Division Commission on Ground Disposal of Radioactive Waste, Princeton University, Princeton, New Jersey)
51. J. R. Horan, AEC, Idaho
52. J. H. Horton, SRI
53. J. F. Honstead, Hanford
54. E. R. Irish, Hanford
55. A. A. Jonke, ANL
56. K. K. Kennedy, ICPP
57. W. J. Kaufman, (U. of California, Berkeley)
58. S. Lawroski, ANL
59. B. M. Legler (ICPP)
60. J. A. Lieberman, AEC, Wash.
61. J. A. McBride, ICPP
62. J. W. Morris, du Pont, Savannah River
63. R. L. Nace (Water Resources Division USGS, Wash., NAS-NRC)
64. C. M. Patterson, du Pont, Savannah River
65. W. H. Reas, Hanford
66. C. S. Shoup, ORO, AEC
67. L. Silverman (Harvard Graduate School of Public Health)
68. J. I. Stevens, ICPP
69. C. M. Slansky, ICPP
70. V. R. Thayer, du Pont, Wilmington
71. J. Vanderryn, AEC, ORO
72. Abel Wolman (Chm. National Acad. of Sciences, Committee on Waste Disposal, Johns Hopkins)

LIBRARIES

73. Document Reference Section
74-76. Central Research Library
77-81. Laboratory Records
82. ORNL-RC
83-98. OTIE, AEC
99. Research and Development Div. ORO